Chapter III

PARAMETERS AND DESIGN PRINCIPLES OF ASPIRATION COUNTERS

§ 25. CLASSIFICATION OF COUNTER CIRCUIT ARRANGEMENTS

There are many ways in which the measuring capacitor, electrometer and voltage supply can be connected to the counter circuit. The principal circuit arrangement determines the different properties of the counter, and, consequently, the specific choice of a circuit is of great practical importance.

Below, we shall consider the circuit arrangements of integral counters only. However, all considered circuits are also feasible for differential counters.

To provide a basis for the circuit classification it is advisable to specify criteria determining the properties of the counter and to effect a subdivision of all circuits into several groups according to each criterion.

First, we shall subdivide the circuits into two groups, i.e., respectively corresponding to parallel and series connection of the electrometer into the circuits. In the parallel arrangement (Figure 25.1a) the entire voltage of the voltage supply is applied to the electrometer. The current through the collector plate is determined from the rate at which the voltage decreases at the electrometer. This arrangement was utilized in the well-known counter of Ebert/Ebert, 1901, 1905/. The high voltage supplied to the electrometer renders it necessary to use a coarse instrument of low sensitivity. In contemporary counters the series arrangement is used almost without exception (Figure 25.1b). Here it is possible to employ a sensitive electrometer and to carry out the measurements on the basis of the charge accumulation method as well as by the method of the voltage drop across a resistance connected in parallel to the electrometer. The series arrangement was implied in the first two chapters of the present work.

The parallel arrangement is usually referred to in the literature as the circuit based on the "discharge method," and the series arrangement – that based on the "charging method." However, these names are not always used consistently. In some cases the series arrangement was called the circuit based on the "discharge method" /Nolan, J.J., Nolan, P.J., 1935; Reinet, 1958, 1959a/.

The inconsistency in the terminology "charge method" and "discharge method" is partly due to the fact that these names do not describe the essential feature of the method and are, consequently, rather arbitrary. In fact, as charge accumulates, the measuring capacitor discharges in

both methods, and the electrometer in the series arrangement can be charged or discharged depending on the initial charge.

Sometimes the parallel arrangement is called the circuit with the low-sensitivity electrometer, and the series arrangement the circuit with the high-sensitivity electrometer.

Secondly, we shall subdivide all circuit arrangements into three groups depending on the ground connection. If the point c is grounded (Figure 25.1), we have a circuit with a grounded repulsive plate. In this circuit the edge effect causes an increase in the current through the collector plate. When grounding the point a, we obtain a circuit with a grounded collector plate. In this case the edge effect causes a decrease in the current through the collector plate. Grounding the circuit at point b gives a circuit arrangement with an intermediate grounded point, which is the most general arrangement and which includes the two preceding schemes as limiting cases /Tammet, 1962b/.

Sometimes the "charging method" and the "discharge method" are distinguished according to the choice of the ground connection, i.e., the first applies to the method of the grounded repulsive plate and the second to the method of the grounded collector plate.

Thirdly, the circuit arrangements are subdivided according to the geometry of the measuring capacitor. Here, there are also three principal variants: the cylindrical capacitor with an inner collector plate, the parallel-plate capacitor, and the cylindrical capacitor with an outer collector plate.

The classification scheme shows the classification of the circuit arrangements of counters.

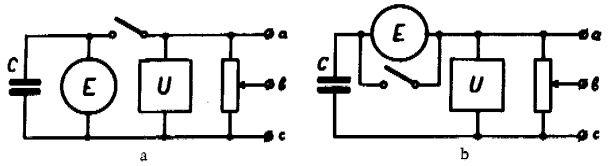

FIGURE 25.1. Principal circuit arrangements of a counter:

C – measuring capacitor; E – electrometer; U – voltage supply.

Of the 18 possible circuit arrangements, only the five indicated by lines in classification scheme 25.1 are applied in practice. Let us briefly consider these variants.

1. The parallel arrangement. Since only one variant of the parallel arrangement has practical application, there is no need to specify further the name. The usual name "discharge method" can be applied only to the parallel arrangement, although in the literature this is not always the case. The use of the parallel arrangement was described already in the first papers on the study of the electrical conductivity of air/Wiedemann, 1885; Elster, Geitel 1899/. The most widely known counters are those of Ebert/Ebert 1901, 1905; Lutz, 1909/ and Gerdien/ Gerdien, 1905a, 1905b/. In the parallel arrangement the instability of the voltage supply cannot affect the measuring result, since the voltage supply is turned off

during the charge accumulation cycle. However, because of the low sensitivity of the electrometer, this advantage has no practical value. Currently, the parallel arrangement is rarely used and is mainly of historical significance.

Classification scheme 25.1

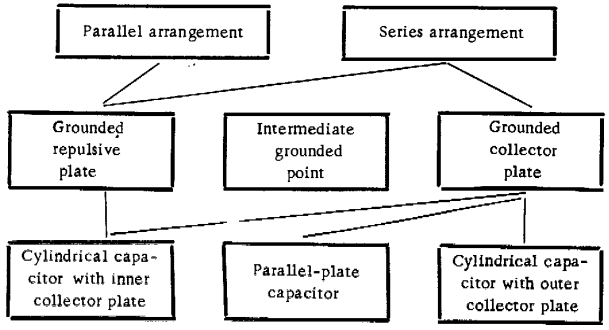

2. The series arrangement with a grounded outer plate. The inner plate is the collector plate. To prevent ambiguity, the classification according to the "discharge method" and "charging method" should not be used here. The series arrangement with the grounded outer plate was used already in the first aspiration counter /Thomson, J.J., Rutherford, 1896; McClelland, 1898; Rutherford, 1899/. Later, it gained wider application /Nordmann, 1904a, 1904b; Baranov, 1925; Israël, 1931; Nolan, J.J., Nolan, P.J., 1935; Weiss, Steinmauer, 1937; Schaffhauser, 1952; Gubichev 1955; Reinet, 1958, 1959a; Hock, Schmeer, 1962/. In some of the above works the series arrangement with the grounded outer plate was erroneously regarded as a new method. The series arrangement with a grounded outer plate readily enables the suppression of the edge effect and has been used over the last years.

3. The series arrangement with a grounded inner collector plate. This is usually called the arrangement based on the "method of charging." The series arrangement with the grounded inner collector plate is the most widespread. Among the first works in which this arrangement was described, we shall cite the following: /Zeleny, 1901; Kähler, 1903; Bloch, 1904; Becker, 1909; Lenard, Ramsauer, 1910; Swann, 1914c/. A disadvantage of this arrangement lies in the complications which result from the edge effect.

4. The series arrangement with a grounded outer collector plate enables us to suppress the edge effect. However, it is relatively seldom used /McClelland, Kennedy, 1912; Nolan, J.J., Nolan, P.J., 1930, 1931; Weger, 1935a; Israël, 1937; Siksna, 1961a/.

5. The parallel-plate measuring capacitor was used exclusively in the series arrangement with a grounded collector plate. The parallel-plate capacitor was employed in differential counters /Nolan, J.J., 1919; Erikson, 1921, 1922, 1924, 1929; Nolan, J.J., Harris, 1922; Chapman, 1937; Daniel, Brackett, 1951; Hewitt, 1957/. In integral counters the parallel-plate capacitor was seldom used /McClelland, Kennedy, 1912; Nolan, J.J., Boylan, Sachy, 1925; Beckett, 1961/.

Of some interest are also the series arrangement with a grounded repulsive plate in a parallel plate capacitor and the three variants of the series arrangement with an intermediate grounded point. The remaining nine possible variants of the principal circuit arrangements are of no practical significance whatever.

§ 26. CURRENT MEASUREMENT BY THE CHARGE ACCUMULATED IN A CAPACITOR

The current through the collector plate of an integral counter is usually of the order of $10^{-14}-10^{12}$ A. In differential counters one sometimes must record currents not exceeding $10^{-16}-10^{-15}$ A. Direct methods of current measurement via the magnetic field effects do not ensure the required sensitivity. Consequently, in aspiration counters indirect measurements are used which are based on the conversion of the measured current into voltage, which is then recorded by means of an electrometer. The circuit diagram for converting the current into voltage, when connecting the electrometer in series with the measuring capacitor, is shown in Figure 26.1. Let us combine the internal capacitance of the measuring capacitor, the electrometer capacitance and parasitic capacitances and denote this as the total capacitance C_0. In the same way the resistance R_0 includes all the leakage resistances in parallel with the electrometer.

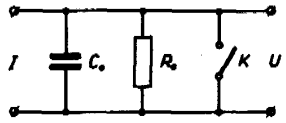

FIGURE 26.1. Circuit diagram for converting current into voltage.

Let the switch K be opened at time $t=0$. Assuming that the current I is constant, we shall represent the time dependence of the voltage by

$$U = IR_0\left[1-\exp\left(-\frac{t}{\tau}\right)\right], \qquad (26.1)$$

where $\tau = R_0C_0$ is the time constant. Of practical importance are only two segments of the function $U(t)$: the initial segment $t \ll \tau$, in which $U \approx \frac{I}{C_0}t$, and the steady-state segment $\tau \ll t$, in which $U \approx IR_0$. Correspondingly, the current measurement method based on the charge accumulated in a capacitor and the current measurement method via the voltage drop across a resistance are distinguished.

In the method of charge accumulation the resistance R_0 should be as large as possible. The largest value of R_0 is restricted by the leakage resistance R_p of the insulators. Since the current is calculated via

$$I = \frac{UC_0}{t}, \qquad (26.2)$$

the occurrence of the resistance R_p causes an error, the relative value of which in the first approximation is $t/2\tau$. If the electrometer is characterized by the limiting error ΔU in the voltage, then the limit of the relative error of current measurement is

$$\delta_I = \frac{t}{2R_pC_0} + \frac{C_0\Delta U}{It}. \tag{26.3}$$

Here it is assumed that the exact value of the capacitance C_0 is known.

The charge accumulation time t is chosen in such a way that the required measurement accuracy is achieved. The shorter of the two solutions of equation (26.3) is

$$t = R_pC_0\delta_I\left(1 - \sqrt{1 - \frac{2\Delta U}{IR_p\delta_I^2}}\right) = \\ = \frac{C_0\Delta U}{I\delta_I}\left[1 + \frac{1}{2}\left(\frac{\Delta U}{IR_p\delta_I^2}\right) + \frac{1}{2}\left(\frac{\Delta U}{IR_p\delta_I^2}\right)^2 + \ldots\ldots\right]. \tag{26.4}$$

A measurement with an error not larger than δ_I will be possible only under the condition

$$I \geqslant \frac{2\Delta U}{R_p\delta_I^2}. \tag{26.5}$$

Formula (26.5) determines the lower limit of current measurement for the given electrometer sensitivity.

In the limiting case $R_p \gg 2\Delta U/I\delta_I^2$, the charge accumulation time is given by

$$t = \frac{C_0\Delta U}{I\delta_I}, \tag{26.6}$$

and in the case $R_p = 2\Delta U/I\delta_I^2$

$$t = R_pC_0\delta_I = 2\frac{C_0\Delta U}{I\delta_I}. \tag{26.7}$$

The last formula determines the larges possible charge accumulation time for a given measurement accuracy.

The electrometer sensitivity depends largely on factors which are of a technical nature. There exists, however, a lower error limit, determined by thermal fluctuations. The determination of thermal fluctuations should be carried out separately for two measuring methods, i.e., for the fixed-zero and the zero-drift method.

In the method of the fixed zero only one electrometer reading is taken. The initial instant $t = 0$, $U = 0$ is taken as the instant at which the switch is opened. After opening the switch a residual charge will remain in the capacitance C_0, which is included in the measurement results. This is a serious disadvantage of the fixed-zero method. A proper switch design helps to decrease the charge generated by the contacts /Shulman, Shepsenvol, 1950; Polonnikov, 1960/, but the thermal noise level still remains the decisive factor for the limit of this charge. The variance of the thermal voltage jumps when opening the switch is simply

$$\sigma_U^2 = \frac{KT}{C_0}. \tag{26.8}$$

Since this quantity equals the variance of the steady random process of the R_pC_0 circuit, the voltage variance at $I = 0$ is determined by expression (26.8) independently of the time after the switch is opened.

Using expression (26.2), we obtain the mean-square error of the measured current

$$\sigma_I = \frac{\sqrt{KTC_0}}{t}. \tag{26.9}$$

In practical applications ($T = 288°K$) this formula becomes

$$\sigma_I(a) = \frac{6.3 \cdot 10^{-17}\sqrt{C_0(\text{nF})}}{t(\text{sec})} \tag{26.10}$$

In the zero-drift method two readings are taken: U_1 at the instant t' and U_2 at the instant $t + t'$ after opening the switch. The current is calculated from the ratio $I = C(U_2 - U_1)/t$. To determine the error we consider the case $I = 0$. The variance of the difference $U_2 - U_1$ is $\sigma^2_{U_2-U_1} = \sigma^2_{U_2} + \sigma^2_{U_1} - 2R_{1,2}\sigma_{U_1}\sigma_{U_2}$, where $R_{1,2}$ is the correlation coefficient between the voltages U_1 and U_2. For the thermal noise of the RC circuit /Lebedev, 1958/ we obtain

$$R_{1,2} = \exp\left(-\frac{t}{\tau}\right). \tag{26.11}$$

The variances $\sigma^2_{U_1}$ and $\sigma^2_{U_2}$ are expressed by formula (26.8). The mean-square error of the current measurement equals the ratio $C_0\sigma^2_{U_2-U_1}/t$. With the approximation $t \ll \tau$, calculation yields

$$\sigma_I = \sqrt{\frac{2KT}{R_pt}}. \tag{26.12}$$

For actual calculations ($T = 293°K$) this formula is written in the form

$$\sigma_I(a) = \frac{9 \cdot 10^{-17}}{\sqrt{R_p(\text{Tohm})t(\text{sec})}} \tag{26.13}$$

In the zero-drift method the voltage sensitivity of the electrometer depends on the charge accumulation time. The last term of expression (26.3) which is inversely proportional to time vanishes. We must therefore reassess some of the statements made at the beginning of the present section. Solving the problem of the minimum error δ_I, we obtain the charge accumulation time ensuring the greatest current sensitivity in the zero-drift method

$$t = \frac{2}{3}R_pC_0\delta_I. \tag{26.14}$$

The minimum value of the current measured at 99% confidence level with an error not greater than δ_I is

$$I_{min} \approx \frac{6}{R_p \delta_I^{1.5}} \sqrt{\frac{KT}{C_0}}. \qquad (26.15)$$

In practice ($T = 287°K$), the last formula has the form

$$I_{min}(a) \approx \frac{3.8 \cdot 10^{-13}}{R_p(\text{Tohm})\sqrt{C_0\,(\text{nF})}\ (100\,\delta_I)^{1.5}} \qquad (26.16)$$

The above expressions determine the theoretical limit of current measurement only when neglecting the correction for leakage. When this correction is included, it is possible to measure a weaker current. However, at present, even the limit defined by formula (26.15) is not reached in practice because of the occurrence of distorting factors of another origin, for example, the additional current generated by the insulators of the electrometer and the measuring capacitor.

A comparison of the thermal noise in the methods of the fixed and the drifting zero points to marked advantages of the latter. For example, under the conditions $C_0 = 100$ nF, $R_p = 10^{16}$ ohm, $t = 100$ sec, the mean-square error due to thermal fluctuations is $6.3 \cdot 10^{-18}$A for the fixed zero and $9 \cdot 10^{-20}$A for the drifting zero.

In some cases the pulse method is used /Schulman, Shepsenvol, 1950; Arabadzhi, Rudik, 1963/, which is sometimes called the integration method. In the pulse method the zero is fixed. The charge accumulates on the capacitance C_1, which is not connected to the electrometer. The variance of the accumulated charge under the operating conditions $I = 0$ is KTC_1. At the end of the cycle the capacitance C_1 is connected in parallel with the input RC circuit of the electrometer, which records the voltage pulse. If the input capacitance of the electrometer is C_2, then the variance of its fluctuating charge prior to connecting capacitance is KTC_2. The sum of the variances of the charges on C_1 and C_2 coincides with the variance of the steady-state process of the circuit after connecting the capacitance C_1 to the electrometer. Consequently, the variance of the measured current does not depend on the time during which a voltage reading is performed, provided this time is considerably smaller than the time constant of the electrometer input. The mean-square error is expressed by formula (26.9), assuming $C_0 = C_1 + C_2$.

The advantage of the pulse method is that the electrometer can be used with a relatively small input resistance without limiting the current sensitivity. The disadvantage lies in the necessity of choosing the charge accumulation time beforehand without knowing the value of the measured current. In other respects the pulse method is similar to the usual method of charge accumulation with a fixed zero.

§ 27. CURRENT MEASUREMENT BASED ON THE VOLTAGE DROP ACROSS A RESISTANCE

In this method the operating conditions correspond to $t \gg \tau$. The current is calculated from Ohm's law $I = U/R$. In order to ensure

measurement accuracy and to shorten the voltage stabilization time, a special shunt resistance R, considerably smaller than the leakage resistance R_p of the insulators, is inserted into the circuit.

In the preceding section we neglected the error in the determination of the capacitance C_0. With regard to the leakage resistance R this was unjustified. The stability and measurement accuracy of high resistances employed in counters are smaller than the stability and measurement accuracy of small capacitances by more than one order of magnitude. The relative error δ_R is included in the error of the measurement results. To simplify the error calculation, we shall introduce the special notation $\delta_I' = \delta_I - \delta_R$ for the error due to other causes. In the case at hand this error is given by

$$\delta_I' = \frac{\Delta U}{IR} + \exp\left(-\frac{t}{\tau}\right). \qquad (27.1)$$

The measurement can be performed if

$$I > \frac{\Delta U}{R\delta_I'}. \qquad (27.2)$$

The time lost for obtaining a reading is

$$t = \tau \ln \frac{1}{\delta_I' - \frac{\Delta U}{IR}}. \qquad (27.3)$$

It is advisable to select the resistance R in such a way that this time is minimized. Suppose that ΔU does not depend on the resistance R. The solution of the extremum problem $dt/dR = 0$ can be written in the form

$$R_{opt} = \frac{\Delta U}{I\delta_I'} f_{opt}(\delta_I'). \qquad (27.4)$$

$f_{opt}(\delta_I')$ cannot be expressed in terms of elementary functions. Some values found by numerical methods are listed in Table 27.1.

In the interval $2 \cdot 10^{-5} < \delta_I' < 0.45$ the function $f_{opt}(\delta_I')$ is approximated with an error less than 1% by the expression

$$f_{opt} \approx 1.180 + 0.79\ \delta_I' - \frac{0.00048}{0.005 + \delta_I'}. \qquad (27.5)$$

At optimum resistance and for the initial condition $U_{t=0} = 0$ the measurement time is

$$t = \frac{C_0 \Delta U}{I\delta_I'} \frac{f_{opt}(\delta_I')}{f_{opt}(\delta_I') - 1}. \qquad (27.6)$$

Comparing the above expression with formula (26.6), we can see that the measurement time in the method of the voltage drop across a resistance is at least $f_{opt}/(f_{opt} - 1)$ times larger than the measurement time in the method of charge accumulation. Several values of the function $f_{opt}/(f_{opt} - 1)$

are listed in Table 27.1. The above statement holds if $U_{t=0} = 0$. However, the stabilization time of a reading having the required accuracy exceeds the measurement time in the method of charge accumulation also in the case of a sudden change in the current.

TABLE 27.1

$\delta_I'(\%)$	t_{opt}	$\frac{t_{opt}}{t_{opt}-1}$	$\delta_I'(\%)$	t_{opt}	$\frac{t_{opt}}{t_{opt}-1}$	$\delta_I'(\%)$	t_{opt}	$\frac{t_{opt}}{t_{opt}-1}$
0	1	∞	0.3	1.13	9.0	5	1.21	5.8
0.001	1.07	15.2	0.5	1.14	8.4	10	1.26	4.9
0.005	1.08	13.5	1	1.15	7.6	20	1.34	4.0
0.02	1.09	12.0	1.5	1.16	7.2	30	1.41	3.4
0.1	1.11	10.2	2	1.17	6.9	40	1.49	3.0
0.2	1.12	9.4	3	1.19	6.3	50	1.60	2.7

In order to determine the limiting accuracy of the method of the voltage drop across a resistance, we shall consider the thermal fluctuations of the current. Let us suppose that the output signal of the electrometer is smoothed by an integrating RC circuit having a time constant τ_2. In the absence of such a circuit, we must set $\tau_2 = 0$. The insertion of the output smoothing circuit increases the inertia but at the same time decreases the effect of thermal fluctuations on the measurement result, which in certain cases may be advantageous. The mean-square fluctuation of the recorded current, derived from the signal fed into the electrometer, is given by

$$\sigma_I = \sqrt{\frac{KTC_0}{\tau_1(\tau_1+\tau_2)}}, \tag{27.7}$$

where τ_1 is the time constant of the input circuit. In practice, this formula takes on the following form ($T = 288°K$):

$$\sigma_I(a) = 6.3 \cdot 10^{-17} \sqrt{\frac{C_0(\text{nF})}{\tau_1(\text{sec})\,[\tau_1(\text{sec}) + \tau_2(\text{sec})]}} \tag{27.8}$$

A comparison of formulas (27.8), (26.9) and (26.12) shows that the sensitivity limit of the method of the voltage drop across a resistance is of the same order of magnitude as the sensitivity limit of the method of charge accumulation with a fixed zero but is lower than the sensitivity of the zero-drift method.

When using the output of the integrating circuit, the problem of selecting the optimum ratio of the time constants τ_1 and τ_2 arises. This problem

should be solved in such a way that for a given thermal noise level σ_I a minimum stabilization time of the reading can be achieved with an error δ. The error is determined from the equation of the transient process

$$\left.\begin{aligned} \delta &= \frac{\tau_1}{\tau_1-\tau_2}\exp\left(-\frac{t}{\tau_1}\right) - \frac{\tau_2}{\tau_1-\tau_2}\exp\left(-\frac{t}{\tau_2}\right);\ \tau_1 \neq \tau_2 \\ \delta &= \left(1+\frac{t}{\tau_1}\right)\exp\left(-\frac{t}{\tau_1}\right);\ \tau_1 = \tau_2 \end{aligned}\right\}. \tag{27.9}$$

The problem of determining the optimum operation conditions reduces to finding the minimum of the function

$$\delta(\alpha) = \frac{(1-\alpha)\exp\left(-\frac{\vartheta}{\sqrt{1-\alpha}}\right) - \alpha\exp\left(\frac{\vartheta\sqrt{1-\alpha}}{\alpha}\right)}{1-2\alpha}, \tag{27.10}$$

where

$$\alpha = \frac{\tau_2}{\tau_1+\tau_2} \tag{27.11}$$

and

$$\vartheta = \frac{\sigma_I}{\sqrt{KTC_0}}\ t. \tag{27.12}$$

The optimum value of the parameter α is determined by a numerical solution of the corresponding equation. Some results obtained in these calculations are listed in Table 27.2.

TABLE 27.2

δ	α_{opt}	$\vartheta_{\alpha=\alpha_{opt}}$	$(\Delta\vartheta/\vartheta)_{\alpha=0}$	$(\Delta\vartheta/\vartheta)_{\alpha=0.5}$
0.02%	40%	7.5	14%	5%
0.13%	37%	6.0	11%	7%
0.43%	34%	5.0	9%	8%
1.2 %	30%	4.2	6%	10%
2.8 %	25%	3.4	4%	12%
4.7 %	20%	3.0	2%	15%
9.3 %	10%	2.4	0.5%	19%
13.5 %	0%	2	0%	24%

The table also gives the relative increase in the current stabilization time as compared with the optimum operating conditions at $\alpha = 0$ and $\alpha = 0.5$.

Despite the inertia and the lower sensitivity, the method of measuring the voltage drop across a resistance is often more convenient than that of charge accumulation. This is explained by the fact that in the former case, simple, continuous current recorders can be used. In the

method of charge accumulation an intricate commutation device is required for automatic current recording. The method of charge accumulation with a drifting zero is preferable if a particularly high accuracy or sensitivity is desired. Another advantage of the method of charge accumulation still remains to be pointed out. Commutation of the input circuit ensures in each cycle automatic compensation of the zero drift of the electrometer. In the method of the voltage drop across a resistance the zero drift is very troublesome, so that more stringent requirements must be imposed on the electrometer.

§ 28. SENSITIVITY OF THE INTEGRAL COUNTER

The often used determination of the sensitivity of the measuring instrument as well as the number of scale divisions in a measurement unit is not fully satisfactory. To render this determination more precise one should, in addition, indicate the ratio of a scale division to the possible errors in the measurement result. In essence, the sensitivity of an instrument is uniquely determined by the distribution of measurement errors for small values of the measured quantity. Here, we shall characterize the sensitivity by means of the standard deviation σ_x of the measurement result when the value of the measured quantity x is zero. The term "sensitivity" is taken to mean the ratio of a unit of the measured quantity σ_x or some other quantity which increases with decreasing σ_x. There is no need for a quantitative determination of the sensitivity.

Measurement errors in the absence of air ions are due to several factors:

1) errors in the electrometer readings (instrument error);
2) induced current when measuring the voltage or the capacitance of the measuring capacitor;
3) current noise due to the properties of the insulators.

The errors in the electrometer readings are due to thermal fluctuations and imperfection of the electrometer. The thermal fluctuations of the current were considered in the preceding sections. The imperfection of the electrometer causes an additional error in the voltage, the standard deviation of which will be denoted by σ_{UE}. The latter is a function of time. However, in practical calculations it can be assumed, for simplicity, to be constant.

In the method of charge accumulation with a fixed zero we must, in addition, allow for charges of nonthermal origin, which arise when the contacts are disconnected. The variance of this charge σ_{Qk}^2 is determined by the design of the switch and by internal disturbances.

The variation of the voltage applied to the measuring capacitor induces a current producing a distorting effect /Weger, 1935b/. The same applies to the instability of the capacitance of the measuring capacitor. If the plates of a parallel-plate capacitor are not perfectly parallel, a relative change in the capacitance

$$\delta_C = \frac{\Delta d}{d} \tag{28.1}$$

is induced, where Δd is the variation in the interplate distance. When one of the axes of a cylindrical capacitor is displaced by dr, we obtain

$$\delta_C \approx \frac{2\Delta\, r dr + (dr)^2}{(r_2^2 - r_1^2)\ln\frac{r_2}{r_1}}, \tag{28.2}$$

where Δr is the initial separation between the axes. From expression (28.2) it follows that the stability of the capacitance of a cylindrical capacitor depends strongly on the accuracy of centering the cylindrical plates.

A distorting induced current is also caused by a random variation in the dielectric constant of the air flowing through the measuring capacitor. The induced current is generated also by the rapid drift in the contact potential between the plates of the measuring capacitor. The last two factors are of second-order significance and will not be considered in the following discussion.

The effect of random variations in the supply voltage can be partly compensated by means of special connections. It is therefore useful to introduce the concept of the equivalent fluctuation voltage, which in compensated circuits is correspondingly smaller than the fluctuating component of the voltage supply. When determining the equivalent fluctuation voltage it is advisable to allow simultaneously for the random variations in the capacitance of the measuring capacitor, since relative variations in the capacitance are equivalent in their effect to equal relative variations in the voltage applied to the measuring capacitor.

In the method of charge accumulation the variance of the mean induced current per cycle is

$$\sigma_{IU}^2 = \frac{C^2 U^2 s_{\Delta UC}^2(t)}{t^2}, \tag{28.3}$$

where C is the effective capacitance of the measuring capacitor and $U^2 s_{\Delta UC}^2(t)$ is the variance of the changes in the equivalent fluctuation voltage during time t. The relative variance $s_{\Delta UC}^2(t)$ can be expressed in the form

$$s_{\Delta UC}^2(t) = 2s_{UC}^2[1 - R_{UC}(t)], \tag{28.4}$$

where s_{UC}^2 is the variance of the ratio of the equivalent fluctuating voltage to the mean voltage of the measuring capacitor, and $R_{UC}(t)$ is the correlation coefficient between the equivalent fluctuation voltages at the initial and final instant of the cycle.

The capacitance C_p attenuates the variations in the voltage by a factor of $C/(C + C_p)$ and increases the capacitance of the differentiating circuit. Taking into account the above information, we obtain the expression for the variance of the induced current in the method of the voltage drop across a resistance

$$\sigma_{IU}^2 = \frac{C^2 U^2 s_{\tau UC}^2(\tau)}{\tau^2}, \tag{28.5}$$

where $\tau = RC_0$.

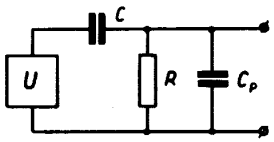

FIGURE 28.1. Circuit arrangement for transferring the fluctuation voltage.

The dependence of $s^2_{\tau UC}(\tau)$ on the correlation function of the fluctuation voltage is very involved. If the effective fluctuation voltage is differentiated with respect to time, then within the limits of small τ and t the induced current is calculated from $I_i = C\frac{dU}{dt}$ and then $s^2_{\tau UC}(t) = s^2_{\Delta UC}(t)$. Within the limits of large values of the time we have $s^2_{\tau UC}(t) = s^2_{UC} = \frac{1}{2} s^2_{\Delta UC}(t)$. In both limiting cases the expression

$$2s^2_{\tau UC}\left(\frac{t}{\sqrt{2}}\right) = s^2_{\Delta UC}(t) \tag{28.6}$$

is valid and can be used for a rough estimation of the ratio of $s_{\tau UC}$ and $s_{\Delta UC}$.

The stability of different voltage sources can be studied experimentally with the aid of the circuit shown in Figure 28.2. The capacitance C must be stable and can have a sufficiently large value, which facilitates the measurements. The additional $R_1C_1 \gg \tau$ circuit is intended to eliminate errors connected with the leakage of the capacitor C. $s_{\tau U}(\tau)$ is determined by the ratio of the instrument reading U_I and the voltage U.

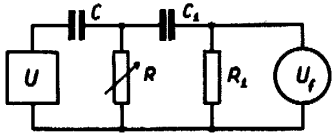

FIGURE 28.2. Circuit arrangement for the determination of $s_{\tau U}(RC)$:

U – voltage source to be investigated;
U_I – instrument for measuring the ultra-low frequency voltage.

The current disturbance generated by the insulators is practically independent of the operating conditions of the measuring capacitor. Experiment shows that this current is inversely proportional to the resistance R_p of the insulators. We shall therefore denote the variance of the insulator current by σ^2_{UR}/R^2_p. The quantity σ_{Up} is usually of the order of a tenth of a volt. During short time intervals the insulator current is so strongly correlated that it may be assumed to be constant.

Leakage through the insulator between the plates will be ignored, since this leakage is fully averted when the insulator is properly designed. Similarly, the errors due to the retarded polarization of the insulators after voltage commutation can be completely eliminated.

When determining the sensitivity one should use as the measured value either the conditional charge density $P = I/\Phi$ or the conditional conductivity $\Lambda = I/4\pi CU$. The variance of the conditional charge density is

$$\sigma^2_P = \frac{\sigma^2_I}{(4\pi k_0 CU)^2}. \tag{28.7}$$

The variance of the conditional conductivity is

$$\sigma^2_\Lambda = k^2_0 \sigma^2_P. \tag{28.8}$$

In order to determine σ^2_I we take the sum of the variance of all the above-considered current disturbances. The following results are obtained.

1. Method of charge accumulation with a fixed zero and the pulse method:

$$\sigma^2_P = \frac{1}{(4\pi k_0 t)^2}\left[s^2_{\Delta UC}(t) + \frac{\sigma^2_{QK} + C^2_0\sigma^2_{UE} + KTC_0}{C^2U^2} + \frac{\sigma^2_{UR}t^2}{C^2U^2R^2_p}\right]. \tag{28.9}$$

2. Method of charge accumulation with a drifting zero:

$$\sigma^2_P = \frac{1}{(4\pi k_0 t)^2}\left[s^2_{\Delta UC}(t) + \frac{C^2_0\sigma^2_{UE}}{C^2U^2} + \frac{2KTt}{C^2U^2R_p} + \frac{\sigma^2_{UR}t^2}{C^2U^2R^2_p}\right]. \tag{28.10}$$

3. Method of the voltage drop across a resistance:

$$\sigma^2_P = \frac{1}{(4\pi k_0 t)^2}\left[s^2_{\tau UC}(\tau) + \frac{C^2_0\sigma^2_{UE} + KTC_0}{C^2U^2} + \frac{\sigma^2_{UR}t^2}{C^2U^2R^2_p}\right]. \tag{28.11}$$

Under certain conditions the above expressions can often be simplified by neglecting one of the terms.

For the condition $t \approx \tau$ formulas (28.10) and (28.11) yield sensitivity values close to one another, since the thermal noise is usually overlapped by the remaining disturbances.

§ 29. CALCULATION OF AIR-ION SPECTRAL CHARACTERISTICS

The partial charge densities, partial conductivities and the spectrum $\varrho(k)$ can be determined from direct measurement only by means of the appropriate calculations. In most of the formulas given in the first chapter, not only air-ion current values are encountered, but also the derivatives of the current with respect to one of operation parameters. This complicates the evaluation of the observations, since the usual measurement methods do not enable us to obtain the continuous function $I(\psi)$, but only a number of isolated points $I(\psi_1), I(\psi_2), \ldots\ldots, I(\psi_n)$.

The graphical methods for determining the quantities expressed in terms of the operator h_ψ were briefly described in § 4. The derivative of the current with respect to ψ can be determined from the curve $I(\psi)$. More detailed information on the graphical method can be found in the literature /Gerasimova, 1939; Imyanitov, 1957; Israël, 1957b/. Complications arise if the curve $I(\psi)$ is to be plotted for the discrete points $I(\psi_n)$ It is somewhat arbitrary to plot a smooth curve. Israël /Israël, 1957b/ pointed out this problem by the question "break point or bend?" To obtain reliable results, the limits of arbitrariness introduced by the evaluation of the observations should be precisely determined. In graphical methods this is quite difficult, as can be seen from the treatment of the nature of the spectrum of heavy air ions in the works /Nolan, J.J., 1916; Blackwood, 1920; Nolan, P.J., 1921; Nolan, J.J., 1923; Nolan, J.J., Sachy, 1927; Boylan, 1931/, and, more recently, /Fuks, 1955; El Nadi, Farag, 1960, 1961/.

The graphical method is inconvenient if the mobility range is large. In practice, one often has to evaluate data on the spectrum of air ions with extreme mobilities with a ratio of 10,000 or more, while on one graph it is difficult to represent a spectrum with a width larger than one order of magnitude. The attempt to give up the linear scale when plotting curves proved unsuccessful, and the ill-considered use of a logarithmic mobility scale /Hoegl, 1963b/ led only to errors.

Interesting ideas on the use of a logarithmic scale may be found in the work /Aoki, Kato, 1954/. However, these ideas still did not enable us to find a method which was less time consuming.

The evaluation of the observations may also be carried out by numerical methods, which were applied in the determination of the partial charge density of light ions /Baranov, 1925; Baranov, Stschepotjewa, 1928; Shchepotieva, 1929/, and recently in the evaluation of spectrum measurements /Hoppel, Kraakevik, 1965/.

The main advantage of numerical methods is that they enable us to estimate the errors in the measurement results, and to determine accurately the uncertainty limits which arise due to the fact that the function $I(\psi)$ is given by a series of points. There are also no difficulties in the case of a large mobility interval. In numerical methods the derivatives are determined from formulas of finite increments. The use of interpolation methods would be unjustified, since nothing besides continuity can be assumed concerning the behavior of the function $\varrho(k)$ /Tammet, 1962d/. Physical considerations also give reason to assume the continuity of the function $I(\psi)$ and its derivatives. Let us stipulate that the points I_n are chosen in a monotonic sequence. If ψ is the voltage, then we shall consider ψ_n with one polarity only. Under these assumptions the following assertions are valid /Tammet, 1962d/:

a) in the interval (ψ_1, ψ_2) there always exists a $\psi = \xi_1$, such that

$$\frac{\partial I(\xi_1)}{\partial \psi} = \frac{I_2 - I_1}{\psi_2 - \psi_1} \tag{29.1}$$

(Lagrange formula);

b) in the interval (ψ_1, ψ_2) there always exists a $\psi = \xi_2$, such that

$$h_\psi I(\xi_2) = \frac{\psi_2 I_1 - \psi_1 I_2}{\psi_2 - \psi_1}; \tag{29.2}$$

c) in the interval (ψ_1, ψ_2) there always exists a $\psi = \xi_3$, such that

$$\xi_3 h_\psi I(\xi_3) = 2\psi_1\psi_2 \frac{\psi_2 I_1 - \psi_1 I_2}{\psi_2^2 - \psi_1^2}; \tag{29.3}$$

d) in the interval (ψ_1, ψ_2) there always exists a $\psi = \xi_4$, and in the interval (ψ_3, ψ_4) a $\psi = \xi_5$, such that

$$\frac{\frac{\partial I(\xi_4)}{\partial \psi} - \frac{\partial I(\xi_5)}{\partial \psi}}{h_\psi I(\xi_4) - h_\psi I(\xi_5)} = \frac{(\psi_4 - \psi_3)(I_2 - I_1) - (\psi_2 - \psi_1)(I_4 - I_3)}{(\psi_4 - \psi_3)(\psi_2 I_1 - \psi_1 I_2) - (\psi_2 - \psi_1)(\psi_4 I_3 - \psi_3 I_4)}; \tag{29.4}$$

e) if ψ_2 is contained in the interval (ψ_1, ψ_3), then this interval contains a $\psi = \xi_6$, such that

$$\xi_6^3 \frac{\partial^2 I(\xi_6)}{\partial \psi^2} = 2\psi_1\psi_2\psi_3 \frac{(\psi_3 - \psi_2) I_1 - (\psi_3 - \psi_1) I_2 + (\psi_2 - \psi_1) I_3}{(\psi_3 - \psi_2)(\psi_3 - \psi_1)(\psi_2 - \psi_1)}. \tag{29.5}$$

With the aid of formulas (29.1) – (29.5) we can calculate all the characteristics, which in the first chapter were expressed in terms of the derivatives of the functions $I(\psi)$ or $P(\psi)$. Formula (29.4) also makes it possible to calculate the mean mobility

$$\bar{k}(k_1, k_2) = \frac{\int_{k_1}^{k_2} k\varrho(k)\,dk}{\int_{k_1}^{k_2} \varrho(k)\,dk} = \frac{\lambda(k_1, k_2)}{\varrho(k_1, k_2)}. \tag{29.6}$$

Below calculation formulas are given for the integral counter and the first-order differential counter in the case of the voltage variation method. The uncertainty of the argument in the formulas of finite differences is interpreted as the error in the measured mobilities. The mobility determined only on the basis of the interval will be denoted by k. The mean mobility of the interval will be denoted by $\bar{k}$ and the maximum relative error corresponding to the uncertainty limits δ_k.

a) The integral counter; calculation of partial charge densities, charge mobilities, and mean mobilities. The voltages U_n are chosen in increasing order: $U_1 < U_2 < U_3 < U_4$.

$$\varrho(\tilde{k}_2, \tilde{k}_1) = \frac{(U_2 - U_1)(U_4 P_3 - U_3 P_4) - (U_4 - U_3)(U_2 P_1 - U_1 P_2)}{(U_2 - U_1)(U_4 - U_3)}, \tag{29.7}$$

$$\lambda(\tilde{k}_2, \tilde{k}_1) = \frac{\Phi[(U_4 - U_3)(P_2 - P_1) - (U_2 - U_1)(P_4 - P_3)]}{4\pi C(U_4 - U_3)(U_2 - U_1)}, \tag{29.8}$$

$$\bar{k}(\tilde{k}_2, \tilde{k}_1) = \frac{\Phi[(U_4 - U_3)(P_2 - P_1) - (U_2 - U_1)(P_4 - P_3)]}{4\pi C[(U_2 - U_1)(U_4P_3 - U_3P_4) - (U_4 - U_3)(U_2P_1 - U_1P_2)]}, \quad (29.9)$$

$$\bar{k}_2 = \frac{\Phi(U_3 + U_4)}{8\pi CU_3U_4}, \quad (29.10)$$

$$\bar{k}_1 = \frac{\Phi(U_1 + U_2)}{8\pi CU_1U_2}, \quad (29.11)$$

$$\delta_{k_2} = \frac{U_4 - U_3}{U_4 + U_3}, \quad (29.12)$$

$$\delta_{k_1} = \frac{U_2 - U_1}{U_2 + U_1}. \quad (29.13)$$

b) The integral counter; calculation of the spectrum $\varrho(k)$. We assume that the condition $U_1 < U_2 < U_3$ is satisfied.

$$\varrho(\tilde{k}) = \frac{8\pi CU_1U_2U_3[(U_3 - U_1)P_2 - (U_3 - U_2)P_1 - (U_2 - U_1)P_3]}{\Phi(U_3 - U_1)(U_3 - U_2)(U_2 - U_1)}, \quad (29.14)$$

$$\bar{k} = \frac{\Phi(U_1 + U_3)}{8\pi CU_1U_3}. \quad (29.15)$$

$$\delta_k = \frac{U_3 - U_1}{U_3 + U_1}. \quad (29.16)$$

In order to obtain the most uniform information for all the investigated mobility intervals and to simplify calculations it is advisable to choose, when possible, the points U_n in a well-defined order. To calculate $\varrho(k_1, k_2)$, $\lambda(k_1, k_2)$ and $\bar{k}(k_1, k_2)$, the U_n should be chosen in pairs, which enable a more distinct determination of the limits of the interval $(\bar{k}_1, \bar{k}_2)$. Here, the ratio U_{n+1}/U_n has for all even numbers one value and for all odd numbers a different value. The smaller of the two ratios determines the error in the mobility, and their product the width of the interval (k_2, k_1). To determine the spectrum $\varrho(k)$ it is expedient to choose U_n with a constant ratio U_{n+1}/U_n. The values of $\varrho(k)$ are calculated on the basis of each three successive U_n, which in the case of m points of the function $P(U)$ always gives $m-2$ points of the function $\varrho(k)$. The relevant calculation formulas are:

a) Choosing

$$\frac{U_4}{U_3} = \frac{U_3}{U_1} = \alpha \quad (29.17)$$

and

$$\frac{U_4}{U_2} = \frac{U_3}{U_1} = \beta, \quad (29.18)$$

we obtain

$$\varrho(\tilde{k}_2, \tilde{k}_1) = \frac{\alpha(P_3 - P_1) - (P_4 - P_2)}{\alpha - 1}, \quad (29.19)$$

$$\lambda(\tilde{k}_2, \tilde{k}_1) = \frac{\Phi[\beta(P_2 - P_1) - (P_4 - P_3)]}{4\pi CU_3(\alpha - 1)}, \quad (29.20)$$

$$\bar{k}(\tilde{k}_2, \tilde{k}_1) = \frac{\Phi}{4\pi CU_3} \frac{\beta(P_2 - P_1) - (P_4 - P_3)}{\alpha(P_3 - P_1) - (P_4 - P_2)}, \quad (29.21)$$

$$\bar{k}_2 = \frac{\Phi(1 + \alpha)}{8\pi CU_4}, \quad (29.22)$$

$$\bar{k}_1 = \frac{\Phi(1 + \alpha)}{8\pi CU_2}, \quad (29.23)$$

$$\delta_{k_2} = \delta_{k_1} = \frac{\alpha - 1}{\alpha + 1}. \quad (29.24)$$

b) Choosing U_1, U_2 and U_3, such that

$$\frac{U_{n+1}}{U_n} = 1 + \delta, \quad (29.25)$$

we obtain

$$\varrho(\tilde{k}) = \frac{4\pi CU_3}{\Phi\delta^2}\left[(2P_2 - P_1 - P_3) + \frac{\delta}{2 + \delta}(P_3 - P_1)\right], \quad (29.26)$$

$$\bar{k} = \frac{\Phi\left(1 + \delta + \frac{1}{1 + \delta}\right)}{8\pi CU_2} \approx \frac{\Phi}{4\pi CU_2}, \quad (29.27)$$

$$\delta_k = \frac{(1 + \delta)^2 - 1}{(1 + \delta)^2 + 1} \approx \delta. \quad (29.28)$$

c) The first-order differential counter with a divided capacitor. $U_2/U_1 = \alpha > 1$.

$$\varrho(\tilde{k}_a, \tilde{k}_b) = \frac{\alpha I_1 - I_2}{(\alpha - 1)\Phi}, \quad (29.29)$$

$$\bar{k}_a = \frac{(\alpha + 1)\Phi}{8\pi(C_1 + C_2)U_2}, \quad (29.30)$$

$$\bar{k}_b = \frac{(\alpha + 1)\Phi}{8\pi C_1U_2}, \quad (29.31)$$

$$\delta_{k_a} = \delta_{k_b} = \frac{\alpha - 1}{\alpha + 1}, \quad (29.32)$$

$$\varrho(k) = \frac{8\pi C_1(C_1 + C_2)U_2}{C_2\Phi^2} \frac{\alpha I_1 - I_2}{\alpha^2 - 1}, \quad (29.33)$$

where

$$k = \frac{(\alpha C_1 + C_1 + \alpha C_2)\Phi}{8\pi U_2C_1(C_1 + C_2)}, \quad (29.34)$$

$$\delta_k = \frac{\alpha(C_1 + C_2) - C_1}{\alpha(C_1 + C_2) + C_1}. \qquad (29.35)$$

When laying out the measurement program, it should be kept in mind, that the errors in the measurement result increase when increasing the accuracy in the mobility determinations by decreasing the constants α and δ. The problem of determining the measurement error will be considered in the following sections. When studying atmospheric ionization with the aid of an integral counter of average sensitivity and accuracy /Reinet, 1956/, the ratios $\alpha = 2$ and $\beta = 5$ are the most suitable. In accordance with the recommendation of the present author such ratios were used in multiannual observations of atmospheric ionization, carried out in Tartu by P. K. Prüller /Prüller, Reinet, 1966/. The evaluation of the observation data was carried out according to formulas (29.19) and (29.21) with the aid of a small desk calculator.

The question of the amount of work necessary to evaluate the observation data should be solved separately for each case with allowance for the actual conditions. One should also consider the possibility of programming the data on a computer, which can considerably increase the efficiency of the computation method. In some cases a graphical method and in other cases a numerical method may appear more convenient. As an example, a comparison of graphical and numerical methods was carried out for the calculation of partial charge densities in an integral counter. The series of limiting mobilities was as follows: 1; 0.5; 0.1; 0.05; 0.01; 0.005; 0.001; 0.0005; 0.0001; 0.00005 $(\frac{cm^2}{V \cdot sec})$. The partial charge densities were calculated in five ranges $\varrho[(0.75 \pm 0.25)\frac{cm^2}{V \cdot sec}, \infty]$, $\varrho[(0.075 \pm 0.025)\frac{cm^2}{V \cdot sec}$, $(0.75 \pm \pm 0.25)\frac{cm^2}{V \cdot sec}]$, etc. The computations were performed by a laboratory assistant, who had no previous experience in the evaluation of observation data by either method. In the numerical method a VMP-2 calculator was employed. To get used to both methods a full working day was spent on each of them. A time check of the control tasks showed that the evaluation of the observation data by means of the graphical method took 2.5 times as long as the evaluation of the same amount of data by the numerical method.

§ 30. ASSESSMENT OF RANDOM ERRORS IN MEASURING THE CHARACTERISTICS OF THE AIR-ION SPECTRUM

Errors in the characteristics of the air-ion spectrum are larger than the errors produced when measuring the conditional charge density. Not only are the direct observation errors significant, but also the instability of the air-ion spectrum during the measurement period. The last factor is irrelevant when the points $I(k_n)$ are taken simultaneously.

The demands imposed upon the accuracy of the error determination are not too high, so that certain simplifying assumptions can be made. Suppose that the parameters of the measuring capacitor are exactly known. If necessary, the omitted error can be separately estimated and added to the result.

Consider the error determination for integral counters. The variance of the errors of the measured quantity x is composed of two terms $\sigma_x^2 = \sigma_I^2 + \sigma_\varrho^2$, where σ_I characterizes the instrument error, and σ_ϱ the error due to fluctuations of the air-ion spectrum with time. To estimate σ_I we assume that the air-ion spectrum is stable. Errors inherent in the instruments are practically independent of one another. Neglecting systematic errors, we can estimate the error in the conditional charge density from formulas (28.9 – 28.11). Assume, for simplicity, that all the P_n appearing in one formula are equal to one another and are denoted by $\bar{P}$. With these assumptions the calculation of the variance σ_I^2 is simple when evaluating the observation data according to formulas (29.19), (29.20) and (29.26).

The fluctuation of the air-ion spectrum with time has the result that the series of successive measurement values $P_1, P_2, \ldots, P_n, \ldots$ do not represent the function $P(U_n)$ for any definite time interval. When estimating σ_ϱ, we assume that the ratio α appearing in formula (29.19) is close to unity. This enables us to estimate the variance of the fluctuations of the differences $\alpha P_1 - P_2$ and $\alpha P_3 - P_4$ from the variances of the differences $P_n - P_{n+1}$, where P_n and P_{n+1} corresponds to the same limiting mobility. Let us adopt the notation $s_\Delta = \sigma_{(P_n - P_{n+1})}/\bar{P}$. To determine s_Δ special supplementary measurements must be performed in which the same time conditions are observed as in the main observation series.

In the same way the variance of the fluctuations of the differences $2P_2 - P_1 - P_3$ appearing in formula (29.26) can be estimated. The corresponding relative standard deviation will be denoted by $s_{\Delta\Delta} = \sigma_{(2P_n - P_{n-1} - P_{n+1})}/\bar{P}$.

Owing to the above simplifications, the formulas for estimating the errors can be written in a simple form, which is convenient for practical calculations. Evaluating the observation data according to formulas (29.19) and (29.20), we obtain

$$\sigma_{\varrho(\bar{k}_1,\ \bar{k}_2)} \approx \frac{\sqrt{2(\sigma_P^2 + \alpha^2\sigma_P^2 + \bar{P}^2 s_\Delta^2)}}{\alpha - 1}, \qquad (30.1)$$

$$\sigma_{\lambda(\bar{k}_1,\ \bar{k}_2)} \approx \frac{k_2\sqrt{(1+\beta^2)(2\sigma_P^2 + \bar{P}^2 s_\Delta^2)}}{\alpha - 1}. \qquad (30.2)$$

Here, we make the additional assumption that the errors in the differences $P_2 - P_1$ and $P_4 - P_3$ are independent of one another and have equal variances. $\bar{P}$ is some mean value of the relative charge densities P_1, P_2, P_3, P_4.

For the evaluation of the observation data according to formula (29.26), assuming that the parameter δ is small, we obtain

$$\sigma_{\varrho(\bar{k})} \approx \frac{\sqrt{6\sigma_P^2 + P_2^2 s_{\Delta\Delta}^2}}{\bar{k}\delta^2}. \qquad (30.3)$$

In first-order differential counters the calculation is similar in all respects. In the differential methods of the second order the estimation of errors is the most simple, since the quantity to be determined is found from the result of one measurement, and, consequently, the fluctuating component of the error drops out.

In practice, the integral method is most often used. Here, the fluctuation of the relative charge intensity is the principal factor determining the measurement accuracy. Random oscillations of the current through the collector plates of the counter were treated in a large number of works /Shepherd, 1932; Baranov, Kravchenko, 1934; Shaffhauser, 1952; Schilling, Carson, 1953; Dessauer, Graffunder, Laub, 1955–1956; Sagalyn, Faucher, 1956, 1957; Siksna, Lindsay, 1961; Siksna, Eichmeier, 1961; Siksna, Schmeer, 1961; Prüller, Reinet, 1966/. However, the authors of these works confined themselves only to citing examples of recordings of the conditional charge density and devoted most of their attention to analyzing the underlying causes of the fluctuations, while leaving the problem of quantitative laws untouched. Only in the work /Collin, Groom, Higazi, 1966/ are quantitative data presented which characterize the relaxation of the autocorrelation function.

To obtain quantitative data on the fluctuations of the conditional charge density of atmospheric air, observations were carried out with the aid of a high-speed counter specially designed for this purpose. This counter was connected in accordance with the circuit arrangement with a grounded inner plate. The parameters and operating conditions of the measuring capacitor are determined by the following parameters: $r_2 = 14$ cm, $r_1 = 2.3$ cm, $l = 45$ cm, $\Phi = 1.5$ m^3/sec, $U = 2$ kV, $k_+ = 5$ cm^2/V·sec. The voltage supply consisted of a stabilized VS-22 rectifier with an additional integrating RC filter ($R = 2$ Mohm, $C = 100\ \mu$F). The absence of disturbances due to random voltage oscillations was established by measurement with the air flow switched on. The filling time $t_0 = 0.02$ sec of the measuring capacitor allows us to assume that the effect of fluctuations of the space charge density on the measurement results is negligibly small. This was verified by special measurements for the operating conditions $U = 0$. The current through the inner plate of the measuring capacitor was measured by the method of the voltage drop across a resistance. A high-speed dynamic electrometer was used. The time constant of the transient process was $\tau = 0.4$ sec. Recording was performed with the aid of the EPP-09M2 electronic potentiometer with a full-scale deflection time of 1 sec. In the experiments, the data of which are given below, the chart speed was 1.33 mm/sec.

The counter was installed in a cabin located not far from Tartu, which is located in the territory of the actinometric station of the Institute of Physics and Astronomy of the AN ESSR. During the experiments wind blew over flat terrain stretching approximately half a kilometer from the cabin. The city was located on the lee side.

The air was sampled at a height of 5 m and was led into the counter through a vertical, wooden channel with a square cross section and a length of 2.6 m. The width of the channel narrowed down from 60 cm at the upper end to 45 cm at the counter inlet. The air was exhausted on the lee side at a distance of 12 m from the counter.

The measurements were performed on July 26 and August 1 and 2, 1963 The positive conductivity was the object of measurement. The trend of the recording was practically independent of the polarity. For a detailed evaluation data of two measurement periods were considered. In the first measurement period – from 19 to 21 hours (local solar time) on August 1 – the intensity of the fluctuations was nearly maximum. The meteorological conditions were as follows: cloudless sky; westerly wind, 2–2.5 m/sec (at a height of 8 m); air temperature at a height of 2 m about 25°C; surface temperature of the soil approximately the same; relative humidity about 50%; pressure 761 mm Hg. During the second measurement interval – from 1 to 2 hours on August 2 – the intensity of the fluctuations was minimum. The meteorological data were: cloudless sky; westerly and southwesterly wind, 2.5–3 m/sec; air temperature at a height of 2 m about 18°C; soil temperature 14°C; relative humidity about 80%; pressure 761 mm Hg. The low intensity of the fluctuations of the conductivity under these conditions was due to a sharp temperature inversion, which led to a decrease in the intensity of the turbulence mixing of the near-ground air layer. The mean conductivity during the second measurement period was two times smaller than during the first period.

The theory of the fluctuation of the air-ion concentration in the atmosphere has not yet been developed. It can be assumed that turbulent mixing /Csanady, 1967/ is the main cause of rapid fluctuations. The initial nonuniformity of the concentration can be explained in terms of the electrode effect.

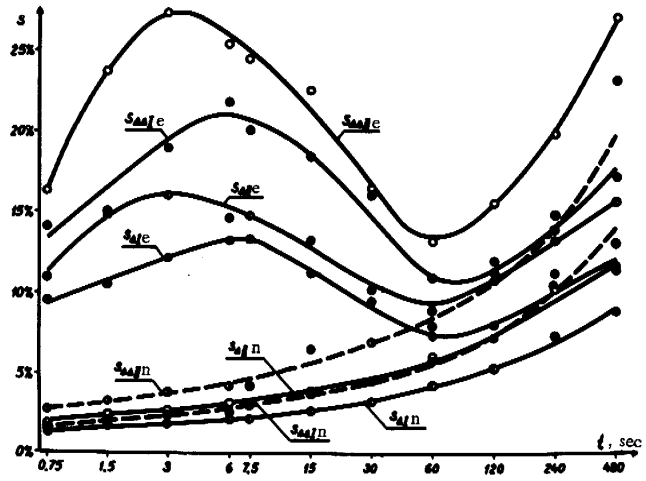

FIGURE 30.1. Results of the investigation of the conductivity of atmospheric air. The subscripts e and n denote the results of evening and night observations.

In the following, the observations taken over the two described measurement periods will be briefly referred to as evening and night observations.

The observation results were evaluated as follows. After recording, the mean conductivities were determined for the consecutive times 0.75, 1.5, 3, 6, 12, 24, 48 sec and 7.5, 15, 30, 60, 120, 240, 480 sec. For the series averaged over $t = 0.75$ sec, $t = 1.5$ sec, etc., each of the 768 sec/t values of mean conductivity were calculated for the evening and the night observations. For the series averaged over $t = 7.5$ sec, $t = 15$ sec, etc., each of the 7680 sec/t values of mean conductivity were calculated for the evening observations and each of the 3840 sec/t values were calculated for the night observations. From the obtained data s_Δ and $s_{\Delta\Delta}$ were determined for different averaging times. The calculations were carried out for two time conditions. For time condition I the differences of the mean conductivities of neighboring averaging intervals were determined. This corresponds to the method of charge accumulation for the condition that the cycles follow one another directly without any time loss during switching. For time condition II the difference of the mean mobilities were determined in unit intervals. This corresponds to conditions under which the time loss during switching of the circuit is the same as the time required for charge accumulation.

The results are graphically represented in Figure 30.1.

Data referring to the averaging time 0.75 sec are somewhat distorted due to the inertia of the recorder.

From the results of the described experiments we arrived at a number of conclusions. As expected, the dependence of $s_{\Delta\Delta I}$, $s_{\Delta II}$ and $s_{\Delta\Delta II}$ on the averaging time basically reiterates the function $s_{\Delta I}(t)$. $s_{\Delta I}$, $s_{\Delta II}$, $s_{\Delta\Delta I}$ and $s_{\Delta\Delta II}$ refer to time condition I and time condition II, respectively. The following relationship holds with slight deviations

$$s_{\Delta II}(t) = 1.26\, s_{\Delta I}\left(\frac{3}{2}t\right). \qquad (30.4)$$

The last result was found from an analysis of the values of the ratio $2s_{\Delta II}(t)/[s_{\Delta I}(t) + s_{\Delta I}(2t)]$. The curve of the frequency of deviations of this ratio from the coefficient of formula (30.4) is given in Figure 30.2, which shows all the results obtained for the averaging times from 3 to 25 sec and from 7.5 to 240 sec.

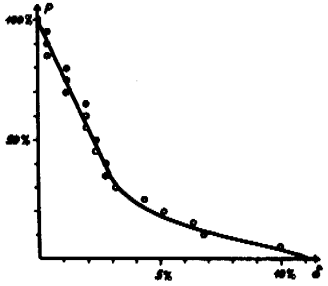

FIGURE 30.2. Error frequency curve of formula (30.4):

p — frequency of errors, exceeding δ.

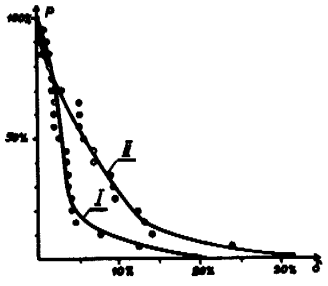

FIGURE 30.3. Error frequency curve of formula (30.5). Roman numerals on the curves denote the operation conditions.

Similar reasoning leads to the formula

$$s_{\Delta\Delta}(t) = s_\Delta(t)\sqrt{4 - 1.6\,\frac{s_\Delta^2\left(\frac{3}{2}t\right)}{s_\Delta^2(t)}}. \qquad (30.5)$$

The frequency of deviations of the experimental values from formula (30.5) is plotted in Figure 30.3.

It is of practical interest to study the dependence of s_Δ on the averaging time. If the fluctuations are small, s_Δ increases monotonically with an increase in the averaging time; this increase is due to the slow fluctuations of the conductivity caused by the variation of the meteorological conditions. Under strong fluctuations, a totally different variation trend of $s_\Delta(t)$ is observed: the curve passes through a maximum for an averaging time between 5 and 10 sec, and through a minimum for an averaging time between 60 and 120 sec, the maximum-to-minimum ratio of the s_Δ-values being equal to 1.9 in our case. The knowledge of the variation trend of $s_\Delta(t)$ is necessary for the correct selection of the charge accumulation time. The results obtained show that the tendency to select a charge accumulation time shorter than a minute seems questionable; it would be better to use a time from one to three minutes. These conclusions are tentative, since they are based on limited data. It seems desirable to include special measurements for the study of the function $s_\Delta(t)$ when planning observatory observations of the ionization of atmospheric air.

The quantitative results obtained in the experiments show that under conditions of small fluctuations (during the night temperature inversion) it is possible to measure the spectrum of light ions by the integral method with a standard deviation of 20% for a half-width of 15% of the mobility uncertainty range. The suitability of night conditions for the study of the spectral distribution of air ions was also mentioned in the paper /Norinder, Siksna, 1953/. Under unsuitable conditions the standard deviation will not drop below 30%, even for a half-width of 30% of the mobility uncertainty range. The detailed study of the spectrum $\varrho(k)$ becomes practically meangingless in this case.

The conclusions made so far are true only insofar as the values found for P_n or $\varrho(k_1, k_2)$, $\lambda(k_1, k_2)$ and $\varrho(k)$ are not subsequently averaged over successive measurements series. If such an averaging is carried out, a higher accuracy is theoretically possible. The reasoning with regard to the selection of the charge accumulation time becomes likewise meaningless. It can, in fact, be easily shown that when the results of n measurement series are averaged, an n-fold reduction in the charge accumulation time will always lead to a reduction in the influence of the fluctuations of P_n on the final result.

The above analysis pertains to the charge accumulation method. In the case of the method of the voltage drop across a resistance, the measurement results will be affected more strongly by the fluctuations of the conventional density. The use of this method for the study of the spectral distribution of air ions by an integral or first-order differential counter is therefore not to be recommended.

A rough estimate of the effect of fluctuations on the result of a measurement by the voltage drop method can be obtained on the basis of the approximate equivalence of the times t and 1.7τ, indicated in the paper /Kagan, 1964/.

§ 31. ELIMINATION OF THE EFFECT OF RANDOM VOLTAGE FLUCTUATIONS ON THE MEASUREMENT RESULTS

The sensitivity of a counter connected in series is limited by the instability of the power source. The dependence of the sensitivity of an integral counter on random fluctuations was examined in § 28. A quantitative analysis leads to the conclusion that the stability of the standard electronic voltage stabilizers is insufficient for measuring the polar charge density of heavy air ions under conditions of natural ionization atmospheric air. A somewhat better stability is achieved by using high-quality batteries, for which $s_{\Delta U}(100\ \text{sec})$ is of the order of 10^{-5}. For $k_0 = 0.0001\ \frac{\text{cm}^2}{\text{V}\cdot\text{sec}}$ and $t = 100$ sec, σ_r, caused by the voltage fluctuations, exceeds 50 elementary charges/cm^3, which is frequently inadmissible. To increase the power stability, it is necessary to use batteries of larger dimensions and weight, which are bulky and inconvenient. It seems therefore preferable to eliminate the effect of the supply voltage fluctuations by means of special circuit arrangements.

The connection of the counter to a bridge circuit (see Figure 31.1) is a known method of compensating the current induced by a change in the supply voltage. Since the type of ground connection used can depend on the specific conditions, no ground connection is indicated in Figure 31.1. The utilization of the bridge circuit in the aspiration counter was already described in /Erikson, 1921/. The bridge circuit can be used with equal success in both the integral and the differential measuring methods. The integral counter is examined below.

In this circuit (Figure 31.1) the electrometer is inserted on the diagonal of the bridge formed by the resistances R_1, R_2 and the capacitances of the measuring capacitor C, and the additional compensation capacitor C_1. Assuming that all the parasitic capacitances are connected in parallel to the electrometer, we have the equilibrium condition

$$\frac{C_1}{C} = \frac{R_1}{R_2}. \tag{31.1}$$

When this condition is satisfied, a change in the circuit supply voltage will not affect the electrometer reading.

The use of a bridge circuit is convenient when the sensitivity increase resulting from the decrease in the variance $s^2_{\Delta UC}$, determined in the bridge circuit by the stability of the bridge equilibrium, exceeds the sensitivity loss caused by the insertion of the shunt capacitance C_1. To increase the sensitivity, the capacitance C_1 should be small. This requires, however, a high supply voltage U_s, which exceeds by a factor of $(1 + C/C_1)$ the voltage of the measuring capacitor.

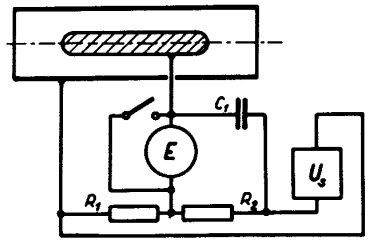

FIGURE 31.1. Counter connection in a bridge circuit.

Consider the problem of the determination of the optimum capacitance $C_{1\,opt}$ (the capacitance giving the minimum error σ_p) corresponding to a given supply voltage U_s of the bridge circuit. The problem has a simple solution only if all the errors except the electrometer error σ_{UE} are neglected. Then

$$C_{1\,opt} = \sqrt{C(C_0 - C_1)}, \tag{31.2}$$

where one starting magnitude is the total capacitance of the isolated system, excluding the capacitance of the compensation capacitor $(C_0 - C_1)$. The influence of the other sources of errors can be estimated in the first approximation

$$C_{1\,opt} \approx (1 + \delta)\sqrt{C(C_0 - C_1)}. \tag{31.3}$$

The expressions for δ are

1) in the method of charge accumulation with fixed zero and the pulse method

$$\delta = \frac{R_p^2\sigma_{QK}^2 + t^2\sigma_{UR}^2 + KT[(C_0 - C_1) + \sqrt{C(C_0 - C_1)}]R_p^2}{2R_p^2\sigma_{UE}^2(C_0 - C_1)[C + \sqrt{C(C_0 - C_1)}]}, \tag{31.4}$$

2) in the method of charge accumulation with drifting zero

$$\delta = \frac{t^2\sigma_{UR}^2 + 2KTR_p t}{2R_p^2\sigma_{UE}^2(C_0 - C_1)[C + \sqrt{C(C_0 - C_1)}]}, \tag{31.5}$$

3) in the method of the voltage drop across a resistance

$$\delta = \frac{\tau^2\sigma_{UR}^2 + KT[(C_0 - C_1) + \sqrt{C(C_0 - C_1)}]R_p^2}{2R_p^2\sigma_{UE}^2(C_0 - C_1)[C + \sqrt{C(C_0 - C_1)}]}. \tag{31.6}$$

The first approximation is adequate for all practical purposes, if $\delta \ll 1$.

The compensation capacitor C_1 must have a high insulation resistance, since leakage causes additional measurement errors. If the admissible value of this error is ΔP, the leakage resistance R_{C_1} must satisfy the condition

$$R_{C_1}C_1 \geqslant \frac{1}{4\pi k_0 \Delta P}. \tag{31.7}$$

The self-discharge time constant of high-quality solid-dielectric capacitors is $10^6 - 10^7$ sec. This is usually insufficient, and special air capacitors have to be used. As in the case of C_1 it is also possible to use the capacitance of the other measuring capacitor, which is not discharged. As a result several other parasitic phenomena are simultaneously compensated /Komarov, Kuz'menko, 1960; Komarov, Kuz'menko, Seredkin, 1961/.

The induced current is best compensated by a differential electrometer, in which the compensating signal can be phase-synchronized with the voltage variation. No voltage division is necessary, and the total voltage of the supply source can be applied to the measuring capacitor, which increases the counter sensitivity. The shunting effect of the compensating capacitor is likewise eliminated. The described circuit differs from the ordinary series circuit in that the other input of the electrometer is connected to the power source via an additional circuit, having the same transfer function as the circuit transmitting the voltage fluctuations through the measuring capacitor to the first input of the electrometer /Jonassen, 1962/.

This principle of compensating power supply fluctuations has been most successfully used in the Imyanitov counter, described in § 10. In this counter compensation is effected without any additional components, using only the symmetry of the system consisting of two measuring capacitors.

Another possibility for eliminating the errors caused by power source instability consists in replacing the power source in the counter circuit by a special reference-voltage capacitor, charged beforehand by the power source /Tammet, 1962b, 1963b/. The condition for a constant self-discharge time of the reference-voltage capacitor coincides with condition (31.7) for the compensation capacitor of the bridge circuit. The capacitance of the reference-voltage capacitor does not shunt the measuring system, and the power source voltage is fully utilized. Furthermore, in this design it is possible to use an ordinary electrometer without differential input. This method, however, possesses a shortcoming. It becomes impossible to effect continuous recording of the current over a long period.

In circuits with a grounded collector plate the reference-voltage capacitor can be connected between the repulsive plate and earth. The capacitance must exceed in this case tens of times the capacitance of the measuring capacitor; otherwise the measurement results will be distorted by the influence of the current generated by air ions of the opposite polarity settling on the repulsive plate. The high capacitance of the reference-voltage capacitor and the higher requirements imposed upon the insulator of the repulsive plate complicate the design of the corresponding counter.

The method of the reference-voltage capacitor is more suitable in the circuit with a grounded outer plate. It is convenient to switch the position between the electrometer and the power source. The reference-voltage capacitor is then connected between the inner plate of the measuring capacitor and the electrometer input (Figure 31.2). During measurements switch K_1 is opened only after the opening of switch K_2, and is closed before the closing of switch K_2. The circuit in Figure 31.2 can be considered from two points of view. If the capacitor C_2 is considered as

the power supply, the circuit then belongs to the series circuit arrangement. The capacitor C_2 can, however, also be considered as an additional element of the electrometer, which, owing to the presence of the dividing capacitor, enables the application of a high direct voltage without impairing the sensitivity to changes in the voltage. According to this interpretation the circuit in Figure 31.2 would seem to belong to the parallel circuit arrangement of the counter. Ignoring this question, we shall designate the circuit in Figure 31.2 as the circuit with a dividing capacitor; this name reflects the function of the capacitor C_2.

The requirement imposed upon the insulation of the dividing capacitor coincides with requirement (31.7).

The capacitance of C_2 is best taken several times larger than the capacitance of the measuring capacitance and electrometer connected in series. A considerable sensitivity loss results when this condition is not fulfilled.

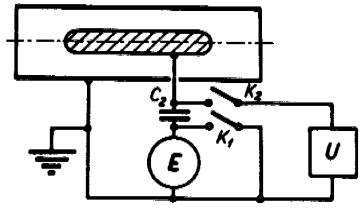

FIGURE 31.2. Circuit arrangement of the counter with a dividing capacitor.

In the circuit of Figure 31.2 the parasitic capacitance C_p is split into the capacitance C_p', consisting of the capacitance of the electrometer and the capacitance of the mounting, and the capacitance C_p'', connected in parallel with switch K_2. In view of the presence of the capacitance C_p'', the dependence of the electrometer readings on random fluctuations of the power source is not completely eliminated, but is only reduced by a factor of C_p''/C. The removal of the capacitance C_p'' is practically impossible, since to ensure the required insulation of the inner plate it is necessary to use two insulating layers with a conducting layer sandwiched between them and connected to the power source. This screens the insulator from the electric field. Otherwise, a considerable leakage and disturbances caused by the retarded polarization of the insulators after power switching is unavoidable.

The influence of the power source instability is completely eliminated in the combined circuit represented in Figure 31.3. The equilibrium condition here differs from condition (31.1) in that the capacitance C is replaced by C_p''. It thus follows that the capacitance of the compensation capacitor C_1 in the bridge circuit with dividing capacitor can be relatively small. The counter sensitivity in this arrangement is therefore higher than in the usual bridge circuit. The bridge circuit with dividing capacitor is particularly convenient for a counter with an interchangeable inner plate of the measuring capacitor, since the balance condition is independent of the effective capacitance.

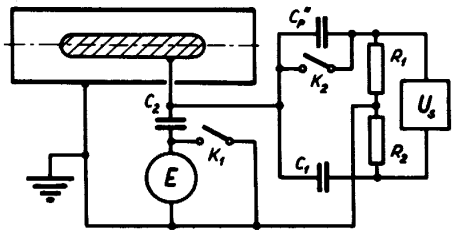

FIGURE 31.3. Combined counter circuit arrangement.

The influence of slow fluctuations in the supply voltage is automatically eliminated in all the modulating counters.

§ 32. PREVENTION OF THE EDGE EFFECT

The edge effect is most simply prevented in counters connected in accordance with the circuit having a grounded outer plate or the circuit with a grounded outer collector plate.

Consider first the circuit with a grounded outer plate. To estimate the edge effect, we use formula (14.5). Since this formula is very approximate, the admissible relative error δ must be specified with sufficient allowance. The effective capacitance of the edge effect must satisfy the inequality

$$C' \leqslant \frac{\delta}{L} C, \tag{32.1}$$

where L is the maximum expected value of the dimensionless ratio $\lambda_2 \Phi / k_0 l(k_0)$.

In order to fulfill condition (32.1) it is necessary to select a sufficiently large distance l' between the end of the inner plate and the plane of the input end of the outer plate perpendicular to the capacitor axis. Experiments on a suitable model were conducted in order to study the dependence of the capacitance C' on the distance l'. The measured parameter was the capacitance C^* between the inner plate of the coaxial capacitor and a large metallic disk placed in the plane of the input end of the outer plate. The disk had an opening at its center coinciding with the inlet opening of the outer plate. The disk was insulated from the outer plate by a thin plexiglass ring. The function $C^* = C^*(l')$ was determined for six replaceable inner plates of different diameter for different end configurations. The The ratio r_2/r_1 had the following values: 1.09, 1.42, 2.09, 3.62, 8.2, 21. The measurement results for a flat end of the inner plate are represented by the empirical formula

$$l' = r_2[\log(r_2/3C^*) - 0.6\log(r_2/r_1)]. \tag{32.2}$$

Formula (32.2) intentionally effects a systematic overestimation of the values of l', since errors in the other direction are more dangerous. The error in the distance l', calculated by this formula, does not exceed $0.1(l' + r_2)$, if $l'/r_2 > 0.5$ and $r_2/r_1 < 20$.

Experiments conducted with inner plates having other end configurations led to similar results, thus making it possible to use formula (32.2) with a certain correction. In the case of an inner plate with a semielliptical end (ratio of the axes 2:1) it is necessary to subtract from the value of l', determined by formula (32.2), the correction $r_1/2$, if $r_2/r_1 \geqslant 2$, or $r_1/4$, if $r_2/r_1 < 2$. For a semispherical end the correction will be $r_1/3$, if $r_2/r_1 \geqslant 2$, and $r_1/5$, if $r_2/r_1 < 2$.

The experimentally confirmed logarithmic relationship expressed by formula (32.2) was theoretically predicted by Grinberg /Grinberg, 1948/. On the basis of these considerations the range of application of formula (32.2) was extended to large ratios l'/r_2, although experimental checks were carried out only up to $l'/r_2 = 3$. The procedure for a quantitative estimate of the length l' is also discussed in the paper /Schmeer, 1966/.

The definition of the capacitance C' is similar to the definition of the capacitance C^*, so that in the design calculation of the counter it is possible to start from the approximation $C' \approx C^*$ and to calculate the required length of the inlet cylinder by formulas (32.1) and (32.2). In the empirical determination of the edge effect current, two- and threefold deviations from the relationship $C' = C^*$ were observed in some counters. However, due to the logarithmic relationship this error is compensated by a small reserve in the length l'.

A sufficiently large length l' contributes also to the damping of external aerodynamic disturbances in the inlet portion of the capacitor. This problem has been little studied, and no specific recommendations can be given. The length l' should not be too large, since this increases the errors caused by the adsorption of air ions.

In the circuit with a grounded outer collector plate the capacitance of the edge effect C_1 has definite significance and can be measured by the usual methods without any additional assumptions. To remove the edge effect, the capacitance C_1 must be selected according to condition (32.1). The dependence of C_1 on l' was studied by model measurements similar to those described above. The measured parameter was the capacitance between the inner plate and the inlet tube of the cylindrical measuring capacitor. The radii of the outer plate and the inlet tube were equal, and the gap between them was equal to $0.05\, r_2$. The experiments were conducted for six values of the ratio r_2/r_1 between 1.09 and 21. The end of the inner plate was provided with replaceable nozzles of different configurations. An empirical formula was established on the basis of the results calculated from (32.2) in such a way that the error cannot take on negative values:

$$l' = r_2[\log(r_2/2C_1) - 0.6\log(r_2/r_1)]. \tag{32.3}$$

The formula represented corresponds to an inner plate with a flat end. The accuracy and applicability limits of this formula are of the same order as formula (32.2). In the case of an inner plate with a semiellipsoidal or semispherical end it is necessary to introduce the same corrections as for formula (32.2).

The required length l' is reduced if a metallic grid is attached to the inlet opening of the outer plate. The screening effect of the grid can only

approximately be estimated by computation methods. On the basis of the known formula of the screening effect of a grid in a parallel-plate capacitor /Kaden, 1950/ it is possible to suggest the following approximate formula for estimating the permeability of a grid transverse to the coaxial capacitor axis:

$$\frac{C_1}{C_{10}} \approx \frac{2h}{3r_2} \log \frac{h}{2\pi r_0}, \qquad (32.4)$$

where C_{10} is the capacitance in the absence of the grid, h the mesh width and r_0 the wire radius.

The coefficient of formula (32.4) was selected empirically. For a grid with $h/r_2 = 0.1$ and $r_0/r_2 = 0.0043$ the measured values of the permeability were up to 15% lower than the values calculated by the formula (for $l'/r_2 > 0.5$). For a grid with $h/r_2 = 0.08$ and $r_0/r_2 = 0.0163$ the permeability is up to 30% lower than the calculated value, owing to the large ratio r_0/h.

Having provided the measuring capacitor with a grid, one should not forget the danger of air-ion adsorption. The dependence of the parameter AC_1/C_{10} on the wire radius is of interest for the selection of the grid size. The calculation shows that AC_1/C_{10} decreases monotonically with a decrease in the wire radius, provided that $h > 6\ r_0$. It is therefore possible to recommend the utilization of the thinnest possible wire, which makes it possible to ensure a smaller adsorption of air ions at a given permeability.

This is illustrated by the following example. If we were to reject the utilization of a grid in the counter described in § 36, the outer plate would have to be lengthened by 30% in order to preserve the previous capacitance of the edge effect.

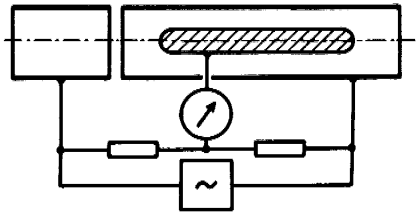

FIGURE 32.1. Bridge for measuring C_1/C.

Corrections for the edge effect can be introduced in the counter with a grounded outer collector plate. For this it is necessary to know the capacitance C_1 with an accuracy higher than that given by formulas (32.3). and (32.4). The ratio C/C_1 is most conveniently measured by an ac bridge (Figure 32.1). When a correction is introduced, it is desirable to fulfill the condition $C/C_1 > k_{max}/k_{min}$, where k_{max} and k_{min} are respectively the maximum and minimum mobilities of the air ions. On the basis of (14.6) we find

$$P(k_0) = P'(k_0) + \frac{C_1}{C} \frac{k_1}{k_0} P(k_1), \qquad (32.5)$$

where $P'(k_0)$ is the value of the conventional charge density distorted by the edge effect, and k_1 is the limiting mobility, exceeding k_{max}.

The suppression of the edge effect is more difficult in counters with a grounded inner collector plate. If the measuring capacitor is not equipped with electrostatic shielding, the edge effect can be estimated from the data given in § 15 of this book. It is not necessary to use electrostatic shielding in all conductivity measuring counters, in which it suffices to determine the critical discharge from the sum of the effective capacitance and the capacitance C' in order to prevent the edge effect. In counters for measuring the partial charge densities the utilization of electrostatic shielding is usually unavoidable.

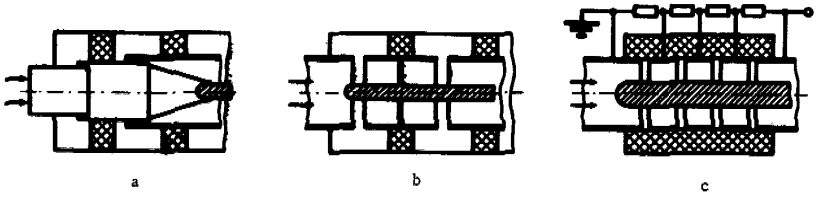

FIGURE 32.2. Electrostatic shields.

The best-known electrostatic shield is due to Swann /Swann, 1914 c/. A drawback of the usual design of the Swann shield (Figure 32.2a) is the air flow expansion upon entering the measuring capacitor, which contributes to the formation of turbulence. The improved variant of the Swann shield, represented in Figure 32.2b /Reimers, 1940; Komarev, Kuz'menko, Seredkin, 1961/, has eliminated this drawback.

In the measuring capacitor with a Swann shield part of the air ions settle on the shield. If the effective capacitance of the measuring capacitor is included the capacitance C' of the respective input device (Figure 15.4e corresponds to Figure 32.2a, and Figure 15.4b to figure 32.2b). The conduction current in the counter with a Swann shield is not strictly linear, but this is of practical importance in rare cases only. The correction C' is usually relatively small and can be considered constant. The effective capacitance of the measuring capacitor is substantial only for air ions of mobility lower than the limiting mobility, and therefore only the range $I/I_0 \leqslant C'/C$ must be allowed for when estimating C' by Figure 15.3.

The Swann shield must reduce the electric field, which penetrates the former until the capacitance C' satisfies condition (32.1). The problem of the longitudinal penetration of an electric field between two coaxial cylindrical surfaces has not been solved. The pattern of field reduction is known only in limiting cases, when the radius of the inner plate is equal to zero or is close to the radius of the outer plate (Grinberg, 1943; Kaden, 1957). In both cases the field strength drops according to a near-exponential law. Using the known theoretical premises and the quantitative relationships established on the basis of the experiments described in connection with formulas (32.2) and (32.3), we suggest the following approximate formula for estimating the necessary length of the Swann shield:

$$l_S = [0.75(r_2 - r_1) + 0.25(r_2 - r_1)^2/r_2]\log(r_2 L/2C\delta). \qquad (32.6)$$

If the inner plate does not penetrate into the shield, we must take $r_1 = 0$. Formula (31.6) has not been checked by direct experiments, and it should therefore be used with certain caution. We have stated it here because no other methods exist for calculating the Swann shield.

The electrostatic shield with transition rings /Komarov, 1961/ is not connected with the inner plate of the measuring capacitor and only slightly increases the parasitic capacitance. The effective capacitance of a measuring capacitor with such a shield (Figure 32.2c) is constant. The determination of the number and length of the transition rings must be effected experimentally, in view of the difficulties involved in the theoretical calculation. The shield calculation is simplified if the length of an individual ring exceeds several times the distance $r_2 - r_1$. In this case the ratio of the first (starting from the air inlet) ring to the voltage of the outer plate must be limited by the value $C\delta/C'L$, where C' is the capacitance of the edge effect of the corresponding input device without shield (Figure 15.4b) for $l/l_0 \approx \delta$. The ratio of voltages of adjacent rings, and also the ratio of the voltage of the outer plate to the voltage of the last ring, must be smaller than C_n/C', where C_n is the capacitance between the transition ring and the inner plate. The shield with transition rings is structurally the most convenient for counters with a small ratio of the radii of the measuring capacitor plates.

A similar electrostatic shield was used in the counter with a divided air flow /Yunker, 1940/, but the efficiency of the shield was in this case much lower, due to the absence of the screening effect of the inner plate. The edge effect capacitance in this shielding is determined by the relationship

$$C' = \frac{S}{4\pi l_Y}, \qquad (32.7)$$

where S is the cross-sectional area of the air flow in the shield, and l_Y the shield length.

§ 33. METHODS OF DETERMINATION OF THE EFFECTIVE CAPACITANCE OF THE MEASURING CAPACITOR

The effective capacitance of the measuring capacitor can be either calculated or measured. While calculation is obviously the only means available in the design stage, measurement represents a more accurate procedure, and is accordingly used after the completion of the counter in order to refine the calculated value.

The capacitance of a coaxial capacitor is calculated by the formula

$$C = \frac{l}{2\ln\frac{r_2}{r_1}}, \qquad (33.1)$$

where l is the capacitor length, r_2 the radius of the outer plate, and r_1 the radius of the inner plate. The capacitor length is determined with an accuracy of the order of r_2, which is frequently insufficient /Swann, 1914b/. The manufacture of a coaxial capacitor of the correct length is possible by using equipotential elongations of the inner plate. An equipotential elongation of the input end of the measuring capacitor is admissible only when measuring the conductivity /Cagniard, Lévy, 1946/, a fact restricting the possibilities of this method.

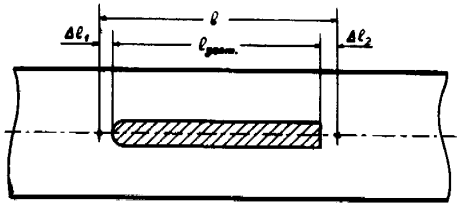

FIGURE 33.1. Effective length of the measuring capacitor.

In § 9 we described a measuring capacitor whose effective capacitance can be accurately calculated (Figure 9.4); this capacitor has, however, a very complex structure.

Formula (33.1) can be considered to be valid in the case of the standard measuring capacitor as well, provided the quantity l is understood as the corresponding effective length /Tammet, 1964a/. In the case of a sufficiently long measuring capacitor, the difference between the effective length and the geometrical length of the inner plate is independent of the plate length, and is uniquely determined by the configuration of the capacitor ends. It is possible to set the points of the effective ends of the inner plate in such a way that the effective length is equal to the distance between them. This is illustrated in Figure 33.1. The effective length is the sum of the geometrical length and the corrections Δl for the two ends.

In the case of equipotential elongation the correction $\Delta l = 0$. The corrections Δl for the other most widely used configurations of the inner plate end were determined by means of model measurements. The experimental setup for these measurements is schematically shown in Figure 33.2. The capacitance between electrodes 3 and 2 is measured by means of a bridge. Electrode 1 serves as an equipotential elongation of plate 3. The electric field is similar to the field in an ideal coaxial capacitor, since the gap between electrodes 2 and 1 was made small. After the removal of electrode 1 from the capacitor, the measured capacitance changed by ΔC. From this we determine the correction for the inner plate which includes the end effect:

$$\Delta l = 2\Delta C \ln\frac{r_2}{r_1}. \qquad (33.2)$$

Such measurements were conducted for six different ratios of r_1/r_2: 0.048, 0.123, 0.276, 0.479, 0.702, and 0.916.

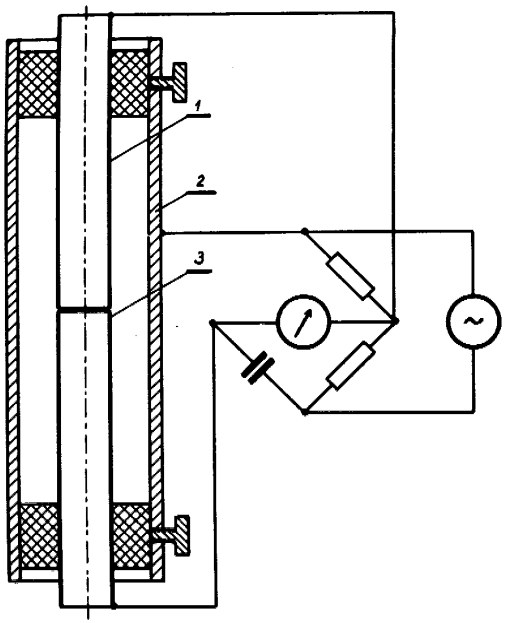

FIGURE 33.2. Arrangement for determining the corrections for the length of the coaxial capacitor:

1 — equipotential elongation; 2 — outer plate; 3 — inner plate.

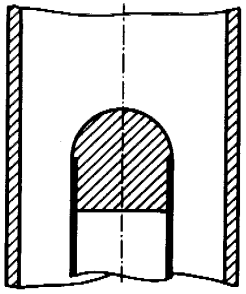

FIGURE 33.3. End of the inner plate with cap.

In order to determine the correction Δl for other configurations of the inner end plate, the change in the capacitance caused by mounting a suitable cap on the end of electrode 3 (see Figure 33.3) was measured. The corrections for an inner plate with a flat end were directly determined by the same method as that used for an inner plate with a hollow end.

The measurement results are plotted in Figure 33.4. The error of curves 1—2 does not exceed 0.01, and that of curves 3—6 does not exceed $0.015 \pm 0.03\ |\Delta l|/r_2$.

The applicability of the curves is restricted by the conditions $l' > 3r_2$ and $l_0 > 3(r_2 - r_1)$, where l' is the distance of the end of the inner plate from the end of the cylindrical portion of the outer plate, and l_0 is the length of the cylindrical portion of the inner plate. According to experimental data given by Schmeer /Schmeer, 1966/, the dependence of ΔC on l' is practically unnoticeable already at $l' = 2r_2'$.

The capacitance of a parallel-plate measuring capacitor is calculated by the standard formulas.

The capacitance of a measuring capacitor with an outer plate and an inner plate can be approximately calculated by the formula

$$C \approx \frac{r_1 l}{2(r_2'' - r_2')}\left[\frac{\ln\frac{r_2''}{r_1}}{\ln\frac{r_2'}{r_1}} + \left(1 + \frac{1}{4}\ln\frac{r_2' r_2''}{r_1^2}\right)\ln\frac{r_2''}{r_2'} + \sum_{n=3}^{\infty}\frac{1}{n \cdot n!}\left(\ln^n\frac{r_2''}{r_1} - \ln^n\frac{r_2'}{r_1}\right)\right], \qquad (33.3)$$

where r_2' is the radius of the outer plate at the thin end and r_2'' at the wide end.

When determining the length of a conic measuring capacitor it is necessary to take into account the corrections for the configuration of the end of the inner plate. With a small error it is possible to use the data of Figure 33.4, taking as r_2 the radius of the outer plate at the end under consideration.

The method which requires the least time for the approximate calculation of the capacitance with an arbitrary plate geometry was described in the paper /Pflügel, 1969/.

The direct measurement of the effective capacitance of the measuring capacitor is complicated by the necessity of eliminating the parasitic capacitances connected in parallel to the measuring capacitor. If this is possible, the parasitic capacitances should be connected in parallel to the null indicator of the bridge. This is achieved in the circuit shown in Figure 33.2, where the capacitance between electrodes 1 and 3 is eliminated. It can happen that the design of the measuring capacitor prevents the realization of such a connection. The effective capacitance can be measured in this case only by means of special methods. One such method is the following. A screen covering the whole inner surface of the outer plate of the measuring capacitor, but insulated from the latter, is manufactured from paper and foil. By connecting the capacitance between the inner plate and the screen in parallel to the null indicator, it is possible to measure the parasitic capacitance C_p. The screen is then

removed, and the total capacitance is measured in the usual way. The effective capacitance is the difference between the total and parasitic capacitances: $C = C_0 - C_p$.

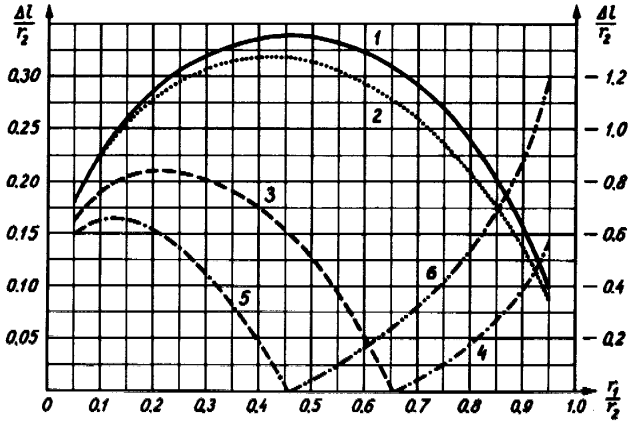

FIGURE 33.4. Curves for determining corrections for the length of the measuring capacitor. The left vertical scale corresponds to curves 1, 2, 3, and 5; the right scale to curves 4 and 6. The curves correspond to the following configurations of the end of the inner cylinder:

1 — plane transverse to the capacitor axis; 2 — transversely cut-off end of a hollow cylinder with wall thickness 0,05 r_2; 3 and 4 — semisphere; 5 and 6 — semi-ellipsoid with major semi-axis equal to the diameter of the inner plate (ratio of the axes 2:1).

§ 34. PRINCIPLES OF THE SELECTION OF THE PARAMETERS AND OPERATING CONDITIONS OF THE INTEGRAL COUNTER

The limiting mobility or the limiting mobility range which must be covered by adjusting the voltage or flow rate must be specified before starting the counter design. The effective capacitance of the measuring capacitor is assumed to be constant for a specific counter, since the adjustment of the effective capacitance is technically difficult and usually not expedient in practice. The specified limiting mobility range can be covered for different selections of the effective capacitance and voltage and flow rate ranges. It is the task of the designer to find the optimal solution.

This problem is complex and cannot be solved in a general form. We shall accordingly restrict ourselves to several particular aspects of practical importance.

We start by examining the dependence of the counter sensitivity on the basic parameters C, Φ, and U for the case of a fixed limiting mobility. Let

the electrometer parameters and the relative instability $S_{\Delta UC}$ or $S_{\tau UC}$ be given. The analysis is based on formulas (28.9) – (28.11). It is easily seen that the sensitivity has an upper limit, determined by the following expressions:

$$\sigma_{P_{min}} = \frac{s_{\Delta UC}(t)}{4\pi k_0 t}, \tag{34.1}$$

when the current is measured by the charge accumulation method, and

$$\sigma_{P_{min}} = \frac{s_{\tau UC}(\tau)}{4\pi k_0 \tau}, \tag{34.2}$$

when it is measured from the voltage drop across a resistance. In order to approach this limit we must increase indefinitely both the flow rate and the voltage.

The flow rate and voltage scale is determined by the absolute critical values Φ_{cr} and U_{cr}, which are the minimum values of these parameters, at which the increase of one of them leads to the limit $\sigma_P^2 = 2\sigma_{P_{min}}^2$. In the charge accumulation method with fixed zero and the pulse method we have

$$\Phi_{cr} = \frac{4\pi k_0}{s_{\Delta UC}(t)} \sqrt{\sigma_{QK}^2 + C_p^2 \sigma_{UE}^2 + KTC_p + \frac{\sigma_{UR}^2 t^2}{R_p^2}} \tag{34.3}$$

and

$$U_{cr} = \frac{\sigma_{UE}}{s_{\Delta UC}(t)}. \tag{34.4}$$

In the charge accumulation method with a drifting zero

$$\Phi_{cr} = \frac{4\pi k_0}{s_{\Delta UC}(t)} \sqrt{C_p^2 \sigma_{UE}^2 + \frac{2KTt}{R_p} + \frac{\sigma_{UR}^2 t^2}{R_p^2}}, \tag{34.5}$$

where U_{cr} is expressed, as before, by formula (34.4).

Here and in what follows we give only the formulas corresponding to the charge accumulation methods. The corresponding expressions for the voltage drop across a resistance are obtained (within the limits of this section) by replacing t by τ, $s_{\Delta UC}$ by $s_{\tau UC}$ and σ_{QK} by 0 in the formulas describing the charge accumulation method with fixed zero and the pulse method.

The effective capacitance does not have an absolute critical value, since for any value of C the unbounded increase of Φ and U leads to the limit $\sigma_P = \sigma_{P_{min}}$.

In practice, the maximum flow rates and voltages are limited by technical considerations. The maximum sensitivity is achieved if the flow rate and the voltage have the highest admissible values and the effective capacitance is selected in accordance with these values. There is no sense in considerably exceeding the critical values of the flow rate and the voltage, although this might be possible in practice.

This recommendation does not apply if the corresponding effective capacitance is beyond the specific technical possibilities. The procedure

in such a case is to select the highest admissible effective capacitance and voltage, and then to determine the flow rate.

The behavior of the function $\sigma_p = \sigma_p(C)$ for a fixed voltage is of interest for the rational selection of the effective capacitance. An unlimited increase in the effective capacitance leads to the value

$$\lim_{C\to\infty}\sigma_p = \frac{\sqrt{\frac{\sigma_{UE}^2}{U^2}+s_{\Delta UC}^2(t)}}{4\pi k_0 t}. \tag{34.6}$$

σ_p^2 attains a double limiting value for the critical value of the effective capacitance $C = C_{crU}$. We obtain

$$C_{crU} = \frac{C_p\sigma_{UE}^2+\frac{KT}{2}}{\sigma_{UE}^2+U^2s_{\Delta UC}^2(t)} + \sqrt{\left(\frac{C_p\sigma_{UE}^2+\frac{KT}{2}}{\sigma_{UE}^2+U^2s_{\Delta UC}^2(t)}\right)^2+\frac{\sigma_{QK}^2+C_p^2\sigma_{UE}^2+KTC_p+\frac{\sigma_{UR}^2t^2}{R_p^2}}{\sigma_{UE}^2+U^2s_{\Delta UC}^2(t)}} \tag{34.7}$$

in the charge accumulation method with fixed zero and the pulse method, and

$$C_{crU} = \frac{C_p\sigma_{UE}^2}{\sigma_{UE}^2-U^2s_{\Delta UC}^2(t)} + \sqrt{\left(\frac{C_p\sigma_{UE}^2}{\sigma_{UE}^2+U^2s_{\Delta UC}^2(t)}\right)^2+\frac{C_p^2\sigma_{UE}^2+\frac{2KTt}{R_p}+\frac{\sigma_{UR}^2t^2}{R_p^2}}{\sigma_{UE}^2+U^2s_{\Delta UC}^2(t)}} \tag{34.8}$$

in the charge accumulation method with drifting zero.

The dependence of the sensitivity on the effective capacitance for a fixed flow rate is of interest for the selection of the parameters of light-ion counters and conductivity-measuring counters. In order to increase the sensitivity it is then necessary to reduce the effective capacitance, while simultaneously increasing the voltage. The sensitivity displays here a dependence on C which is the converse of the preceding case. It is possible in this case as well to indicate a critical capacitance $C_{cr\Phi}$, for which σ_P^2 attains the double limiting value $\lim_{C\to 0}\sigma_P^2$.

In the charge accumulation method with fixed zero and the pulse method we obtain

$$C_{cr\Phi} = \sqrt{2C_p^2+\frac{\sigma_{QK}^2+2KTC_p}{\sigma_{UE}^2}+\left(\frac{KT}{2\sigma_{UE}^2}\right)^2+\left(\frac{\Phi s_{\Delta UC}(t)}{4\pi k_0\sigma_{UE}}\right)^2+\left(\frac{\sigma_{UR}t}{\sigma_{UE}R_p}\right)^2} - \frac{KT}{2\sigma_{UE}^2} - C_p. \tag{34.9}$$

In the charge accumulation method with a drifting zero we have

$$C_{cr\Phi} = \sqrt{2C_p^2+\left(\frac{\Phi s_{\Delta UC}(t)}{4\pi k_0\sigma_{UE}}\right)^2+\left(\frac{\sigma_{UR}t}{\sigma_{UE}R_p}\right)^2} - C_p. \tag{34.10}$$

The counter calculation for the given range of the limiting mobility (k_{min}, k_{max}) is more complex. The counter operating conditions will be described by functions of the limiting mobility. To simplify the calculations, the counter sensitivity can be characterized by the following criterion:

$$\eta = \sigma_p^2(k_{min}) + \Theta^2\sigma_p^2(k_{max}), \tag{34.11}$$

where the parameter Θ is taken equal to the mean ratio $P(k_{min})/P(k_{max})$ is selected on the basis of other considerations. Obviously, for $k_0 = k_{min}$ it is efficient to use the maximum admissible voltage U_{max}, and for $k_0 = k_{max}$ the maximum admissible flow rate Φ_{max}. In the entire range of the limiting mobility the highest sensitivity is achieved when one of these parameters has the maximum admissible value, while the other parameter is determined according to the required limiting mobility. The effective capacitance of the measuring capacitor must be determined from the values U_{max}, Φ_{max} and from some mean value of the limiting mobility. As a function of the effective mobility the criterion η has a minimum, which determines the optimum value C_{opt} of the capacitance.

The condition of the minimum of η leads to the equation of the optimum capacitance

$$1+\frac{C_{opt}}{C_1} = \frac{C_{opt}^3}{C_3^3}+\frac{C_{opt}^4}{C_4^4}, \tag{34.12}$$

where the coefficients C_1, C_3, and C_4 are determined by the following expressions:

1) in the charge accumulation method with fixed zero and the pulse method

$$C_1 = \frac{\sigma_{QK}^2+C_p^2\sigma_{UE}^2+KTC_p+\frac{\sigma_{UR}^2t^2}{R_p^2}}{C_p\sigma_{UE}^2+\frac{KT}{2}}, \tag{34.13}$$

$$C_3^3 = \frac{C_1}{\left(4\pi k_{min}\Theta\frac{U_{max}}{\Phi_{max}}\right)^2}, \tag{34.14}$$

$$C_4^4 = \left(C_p+\frac{KT}{2\sigma_{UE}^2}\right)C_3^3; \tag{34.15}$$

2) in the charge accumulation method with a drifting zero

$$C_1 = C_p+\frac{2KTt}{\sigma_{UE}^2R_pC_p}+\frac{\sigma_{UR}^2t^2}{\sigma_{UE}^2R_p^2C_p}, \tag{34.16}$$

C_3 is expressed in terms of C_1 by formula (34.14)

$$C_4^4 = C_pC_3^3. \tag{34.17}$$

We recall that expressions (34.3), (34.4), (34.6), (34.7), (34.9), and (34.13) – (34.15) can be used in the method of the voltage drop across a resistance, provided we write $\sigma_{QK}=0$ and replace t by τ and $s_{\Delta UC}$ by $s_{\tau CU}$.

If the specific values of the coefficients C_1, C_2 and C_4 are known, equation (34.12) is easily solved by a numerical or graphical method. In the case of a numerical solution it is possible to set $C_{opt}\approx C_4$ in the first approximation.

The above method of calculating the effective capacitance is illustrated below by a particular example with typical values of the parameters. Let us take the following initial values: $k_{min}=0.00033$ cm^2/V·sec, $\Theta=10$, $t=100$ sec, $C_p=10$ cm, $R_p=9\times10^{14}$ ohm, $\sigma_{UR}=300$V, $U_{max}=300$ V, $\Phi_{max}=1000$ cm^3/sec. When using a mechanical electrometer with $\sigma_{UE}=3$ mV, we find $C_{opt}\approx 43$ cm. For a limiting mobility of 1 cm^2/V·sec we obtain $\sigma_p\approx 10$ elementary charges/cm^3, and for the limiting mobility 0.00033 cm^2/V·sec, $\sigma_p\approx 200$ elementary charges/cm^3. Observe that for these initial conditions it is altogether impossible to reduce σ_p below 160 elementary charges/cm^3 for $k_0=0.00033$ cm^2/V·sec by means of an increase in the effective capacitance. If a dynamic electrometer with $\sigma_{UE}=0.3$ mV is used, the optimum capacitance $C_{opt}\approx 90$ cm, and for $k_0=1$ cm^2/V·sec we obtain $\sigma_p\approx 3$ elementary charges/cm^3, for $k_0=0.00033$ cm^3/V·sec $\sigma_p\approx 25$ elementary charges/cm^3. The increase in the optimum capacitance with an increase of the electrometer sensitivity is due to the allowance for the current generated by the insulator. For $\sigma_{UR}=0$ the solution of the problem considered is $C_{opt}\approx 40$ cm, regardless of the electrometer sensitivity.

Specific determinations show that the effective capacitance of the measuring capacitor of many known wide-range counters, selected on the basis of intuitive considerations, is close to the optimum value calculated by the above method. In counters with mechanical electrometers there is a tendency to select a superfluously high effective capacitance, as shown on the basis of the simplified formula of counter sensitivity by /Gubichev, 1960/.

The method described for calculating the optimum effective capacitance should not be considered an absolute and rigorous method. The determination of the optimality on the basis of the minimum of the criterion is in a sense arbitrary and does not reflect all the aspects of the problem. No property of the counter besides the sensitivity was taken into account in the deductions made. The value obtained for C_{opt} should therefore be considered a tentative value, subject to subsequent refinement when selecting the size of the measuring capacitor.

The design calculation of the measuring capacitor is confronted with a number of unsolved and little-studied problems. It is necessary in the first place to solve the problem of adequately neutralizing the distortions linked with the turbulent mixing of air. Two procedures are available to achieve this end. One of them consists in a sufficient decrease of the ratio $l/(r_2-r_1)$. It is then possible to work at $Re>Re_{cr}$, and, as a result, to select a very high air-flow rate and to achieve a high counter sensitivity. This procedure has been little studied, although it seems promising for measurements in the range of high limiting mobilities. A rough estimate

of the maximum ratio $l/(r_2-r_1)$ of the measuring capacitor of the integral counter with turbulent air flow can be made via the formula

$$\frac{l}{r_2-r_1}\leqslant 1000\,\delta^2, \tag{34.18}$$

where δ is the admissible error of the conditional density. The formula was derived on the basis of theoretical considerations and the empirical values at Re = 10,000—16,000, described in the preceding chapter.

The high resolving power necessary for the study of the spectral distribution of air ions according to mobilities is attained only if the turbulent mixing in the measuring capacitor has been sufficiently suppressed. The procedure for reducing the errors connected with the turbulence has likewise been insufficiently studied, although the elimination of the turbulence has been the aim in almost all designs of aspiration counters. To remove turbulent mixing in the measuring capacitor it is necessary to suppress the turbulent fluctuations in the air entering the measuring capacitor, and at the same time to ensure a laminar flow inside the capacitor. The turbulence of the incoming air flow can be suppressed by means of a wire grid /O'Donnel, Hess, 1951; Yaita, Nitta, 1955/. The efficiency of turbulence damping by blowing the air through the grid is calculated by the standard formulas /Batchelor, 1955/ or laminarizing grids /Styro, Matulyavichene, 1965; Dolezalek, Oster, 1965/. However, the use of grids is limited due to the adsorption of air ions. The turbulence can be suppressed to a certain extent by means of an inlet suction nozzle, such as was used in Gerdien's counter /Gerdien, 1905a/. The turbulence is also damped at low Reynolds numbers in a long inlet pipe.

To ensure laminar flow conditions inside the measuring capacitor, the Reynolds number should be sufficiently low. In the determination of the Reynolds number for an annular pipe it is expedient to select $r_2-r_1^2/r_2$ as the characteristic dimension /Lonsdale, 1923/, which ensures the coincidence of the values of the Reynolds number $Re=\Phi/\pi\nu r_2$ for the measuring capacitor and the inlet pipe. The above characteristic dimension was also used in the preceding chapter (formula 21.7). The critical value of the Reynolds number is a function of the ratio r_2/r_1. The data available on this function are not adequate. The only conclusion which can be drawn from the sparse data available /Schiller, 1932; Schlichting, 1959 /is that Re_{cr} increases with a decrease in the ratio r_2/r_1. In some papers /Funder, 1939; El Nadi, Bessa, 1958; Hoegl, 1963b/ the critical value of the quantity $\Phi/\pi\nu(r_2+r_1)$ is taken as constant. This, however, is a very rough approximation. The estimate $(Re=\Phi/\pi\nu r_2)_{cr}\approx 1100(1+r_1/r_2)$ is true only for large values of r_2/r_1, while for low values of this ratio it seems questionable.

Attention should be given to the role played by bars transverse to the flow in the creation of the turbulence /Tammet, 1962c/. If it is impossible to avoid the use of bars, they should be streamlined /Komarov, Kuz'memko, Seredin, 1961/ or made as thin as possible. No turbulence will form behind a cylindrical wire if $r_0<0.01(r_2-r_1)$. This estimate was derived on the basis of the known value of the critical Reynolds number for transverse flow past a cylinder /Landau, Lifshitz, 1954/.

To improve the aerodynamic properties of the measuring capacitor, the outer plate can be made conical. As is known, in a converging flow the laminar flow conditions are preserved for considerably higher flow rates than in a flow of uniform cross section /Loitsyanskii, 1959/.

Experiments on the stability of an air flow in a converging capacitor with flat plates are described in the paper /Hoppel, 1968/ and confirm the above statements. In this study the properties of a conical measuring capacitor were also investigated.

At very low flow rates, air mixing due to heat convection constitutes a problem.

The problem of the maximum admissible field intensity in the measuring capacitor has so far not been solved. A drop in the counter reliability has been observed above 1000 V/cm. This drop is due to the frequent entanglement of microscopic filaments and motes in the capacitor, which leads to the appearance of local discharges and leaks. Obviously, the admissible intensity depends on the linear velocity of the air flow. The value $E_{max} = 1000$ V/cm /Gerasimova, 1939/ corresponds to moderate flow velocities; the increase in the velocity shifts this limit toward higher values. However, the function $E_{max} = E_{max}(u)$, which is highly significant for a substantiated design calculation of the counter, has hardly been studied. The radius of the inner plate must be selected according to E_{max}, and it is expedient to set it equal to the larger of the two solutions of the equation.

$$r_1 \ln \frac{r_2}{r_1} = \frac{U_{max}}{E_{max}}. \tag{34.19}$$

This equation can be solved graphically or numerically.

In the region of high mobilities it is necessary to allow for diffusion, which limits the attainable resolving power of the counter. If, in accordance with /Komarov, Seredkin, 1960; Eichmeier, 1967, 1968/, we determine the resolving power from the relationship

$$R = \frac{k}{\Delta k}, \tag{34.20}$$

where Δk is the minimum difference of the mobilities of two discrete groups of air ions, for which the empirical curve $q(k)$ has two maxima, the resolving power has an upper bound

$$R_d = \frac{1}{2s_{kd}} = \frac{1}{2}\sqrt{\frac{1}{\mu}\frac{qU}{2KT}}. \tag{34.21}$$

The parameter μ was determined in § 19. To increase the limiting resolving power, it is necessary to ensure a sufficiently high value of the voltage, reducing, if necessary, the effective capacitance.

The design calculation for the measuring capacitor on the basis of these considerations is far from perfect. Although there exist some elements of quantitative calculations, the most crucial solutions are based on intuitive considerations, such as the assessment of the value of the initial parameters, and the compromise between accuracy and cost considerations.

The best substantiated method of complete calculation of the optimum design of a counter is based on the minimum cost principle /Tammet, 1963a/. The idea behind one of the variants of calculation by this method consists in the following. Consider a multidimensional space in which the coordinates are determined by the design parameters of the counter. To every point of this space corresponds a specific counter design. Let the functional characteristics of the counter (sensitivity, accuracy, range of limiting mobilities, resolving power, weight, size, etc.) be specified. Set up formulas expressing these characteristics as functions of the design parameters. By substituting the specified values of the functional characteristics into these expressions we obtain equations defining the multidimensional surface of the designs satisfying the specified values. It is possible, in principle, to set up a formula giving the development and manufacturing cost as a function of the design parameters. The optimum design is defined by the coordinates of the point of minimum cost on the surface of the designs satisfying the specified values.

Although designers always solve this problem intuitively, a rigorous mathematical solution is very difficult and laborious. The rapid improvement of the theoretical solutions of individual counter components, such as the electrometer and the power stabilizer, considerably complicates the establishment of cost formulas. The realization of an overall calculation of the optimum design can be useful only when the counter is designed for mass production.

§35. BRIEF SURVEY OF THE DESIGNS OF AIR-ION ASPIRATION COUNTERS

The existing aspiration counters are of the most varied designs. Almost every investigator using the aspiration method of air-ion study introduced some changes in the counter design. The survey given below has no pretentions of completeness. For relatively detailed technical descriptions of the counters we refer to the original papers. Some data on the different counters can also be found in survey papers /Kähler, 1929; Gerasimova, 1939; Torreson, 1949; Imyanitov, 1957; Israël, 1957b; Beckett, 1961; Siksna, 1961a; Minkh, 1963; Knoll, Eichmeir, Schön, 1964/.

The first designs of aspiration counters were described in the papers of J. J. Thomson and his pupils, mentioned in the introduction of this book. We shall briefly describe one of these instruments /McClelland, 1898/, which is of considerable practical interest. This counter is equipped with a cylindrical measuring capacitor with a grounded outer cylinder. The radius of the outer cylinder is 0.85 cm. The counter has two inner cylindrical plates, connected to the electrometer and the power source according to the circuit diagram in Figure 6.1. Both inner plates have a radius of 0.2 cm and are 6.5 cm long. Each of them is fastened to an ebonite insulator by means of a thin transverse bar. The insulator is placed in such a way that its surface is protected from the direct effect of the air flow. The first inner plate is connected to the stabilized power source. The second inner plate is connected to one pair of quadrants of the highly sensitive quadrant electrometer.

The other pair of quadrants is connected to the stabilized power source. Before measurement, both pairs of quadrants are shorted by means of a suitable key. The current is measured by the charge accumulation method. The air is drawn through the measuring capacitor and flowmeter by a water-jet pump. The air-flow rate was 270 cm^3/sec. This instrument was used in laboratory studies.

The scientific and technical level of the instrumentation used by the first investigators of the natural ionization of atmospheric air was much lower than the level attained in the works of the Thomson school. Of greatest historical importance are the instruments of Ebert/Ebert, 1901, 1905/ and Gerdien /Gerdien, 1903, 1905, 1905b/. These two counters are connected according to the parallel circuit arrangement and equipped with electrometers of low sensitivity. The size and operation conditions of the measuring capacitor of the Ebert counter are given by the following figures: $r_2 = 1.46$ cm, $r_1 = 0.25$ cm, $l = 40$ cm, $\Phi = 2000$ cm^3/sec, $U = 200$ V. The Ebert counter was described with negligible alterations in the papers /Lutz, 1909; Speranskii, 1926; Chernyavskii, 1937, 1957/. Gerdien's counter was first intended for conductivity measurement. Its basic parameters are the following: $r_2 = 8$ cm, $r_1 = 0.75$ cm, $l = 24$ cm, $\Phi = 9000$ cm^3/sec. Some features of the Gerdien counter are described in the paper /Hewlett, 1914/.

Subsequently, the method of connecting the counter in series became more widespread. The most important design of the early period is the heavy-ion counter of Langevin and Moulin /Langevin, Moulin, 1907/. This counter employs a highly sensitive quadrant electrometer. The design of the inner-plate insulators are of interest; they are provided with an intermediate metallic layer for protection against leakage. The design of counter insulators with a protective ring was earlier described in the paper /Kähler, 1903/. Measurements by means of the Langevin and Moulin counter have been automized, the electrometer readings being recorded on photographic paper placed on a slowly revolving drum. Another system for the automatic recording of electrometer readings was described still earlier in the paper /Benndorf, 1906/. The evaluation of the recordings of the Benndorf electrograph can be simplfied by using simple apparatus /Tamm, 1960/.

The design of the measuring capacitor of the Langevin-Moulin counter has been used with unessential modifications in the studies /Gockel, 1917; Hess, 1929/.

The next most important improvement in the design of aspiration counters was described in the paper of Swann /Swann, 1914c/, who invented the electrostatic shield.

In the designs of the heavy-ion counter of Langevin and Moulin and the light-ion counter of Swann a level was reached which was comparable to contemporary integral counters equipped with mechanical electrometers. Many known counters and automatic recorders /Kähler, 1930; Torreson, Wait, 1934; Wait, Torreson, 1934; Hogg, 1934; Lutz, 1934, 1936; Grieger, 1935; Greinacher, Klein, 1937; Gerasimova, 1937, 1939, 1941a; Leckie, 1938; Funder, 1939, 1940; Salles, 1942; Reinet, 1956; Saks, 1956; Neaga, Antonescu, 1958/ differ from those described above only by a different combination of the design elements and secondary improvements. Important features of the above-mentioned studies are the use of the method of current measurement from the voltage drop across

a resistance /Wait, Torreson, 1934/, the improvement of the air-supply system and the arrangement of a measuring capacitor with an inlet which opens from below /Hogg, 1934; Leckie, 1938/, the utilization of a flow rate /Grieger, 1935/, the realization of automatic voltage commutation of the measuring capacitor according to a specified program /Saks, 1956/.

The counters described in the works /Thellier, 1933, 1936, 1941; Vasiliu, Calinicenco, Onu, 1954; Vasiliu, Calinicenco, Mateiciuc, 1956/. differ by the utilization of the compensation method of current measurement, in which the electrometer serves as a null indicator.

A peculiar design of the measuring capacitor with increased effective capacitance for a standard size of the instrument is described in the papers /Wolodkewitsch, Dessauer, 1931b; Litvinov, 1938, 1941/.

The paper /Wigand, 1919/ describes the only known attempt to employ an Einthoven galvanometer for the measurement of the current in the counter. In order to increase the current, a large number of measuring capacitors are connected in parallel. Such a method for attaining a high effective capacitance was described earlier in the paper /Kennedy, 1913/. Lately, the parallel connection of several measuring capacitors is again finding application /Mühleisen, 1957b; Hock, Schmeer, 1962; Hoegl, 1963a; Siksna, Eichmeier, 1966/.

An ingenious principle is the operation principle of a simple automatic indicator of ionization anomalies, described in the paper /Milin, Berezina, In'kov, 1954/.

The recent advance in the development of new designs of aspiration counters is due to the application of sensitive cathode electrometers /Godefroy, 1949; Mühleisen, 1957; Dolezalek, 1962a; Hock, Schmeer, 1962; Mendenhall, Fraser, 1963; Hock, 1967/ and dynamic electrometers /Kilinski, 1949, 1953; Callahan, Coroniti, Parziale, Patten, 1951; Curtis, Hyland, 1958; Kraakevik, 1958; Salvador, Masson, 1958; Adkins, 1959; Komarov, Seredkin, 1960; Jonassen, 1962; Saks, 1963; Reinet, Tammet, Salm, 1963; Hoegl, 1963; Reinet, Tammet, Salm, 1967/. A substantial advantage of the cathode and dynamic electrometers consists in the possibility of effecting automatic recording with the aid of the ordinary recording electronic measuring instruments.

In the work /Sozin, 1965/ an instrument is described for measuring the conductivity gradient. In this device a differential cathode electrometer is used.

When the electrometer possesses a high sensitivity, the instability of the power source is of considerable importance. It is necessary in many cases to use bridge and compensation circuits /Komarov, Kuz'menko, 1960; Jonassen, 1962; Reinet, Tammet, Salm, 1963; Kitaev, Kloiz, 1963/. The bridge circuit with a dividing capacitor is also used in the counter designed by the author. The arrangement of the measuring capacitor of this counter is represented in Figure 35.1. The use of an electrometer was described in the paper /Saks, 1963/. A weak flow of specially dried air is blown through the insulated casing. This method of preserving the quality of insulation was treated earlier in the work /Chapman, 1937/.

Although contemporary electrometers enable a nearly complete elimination of leakage via the insulators, quality insulation is still a prerequisite for the suppression of the noise generated by the insulators.

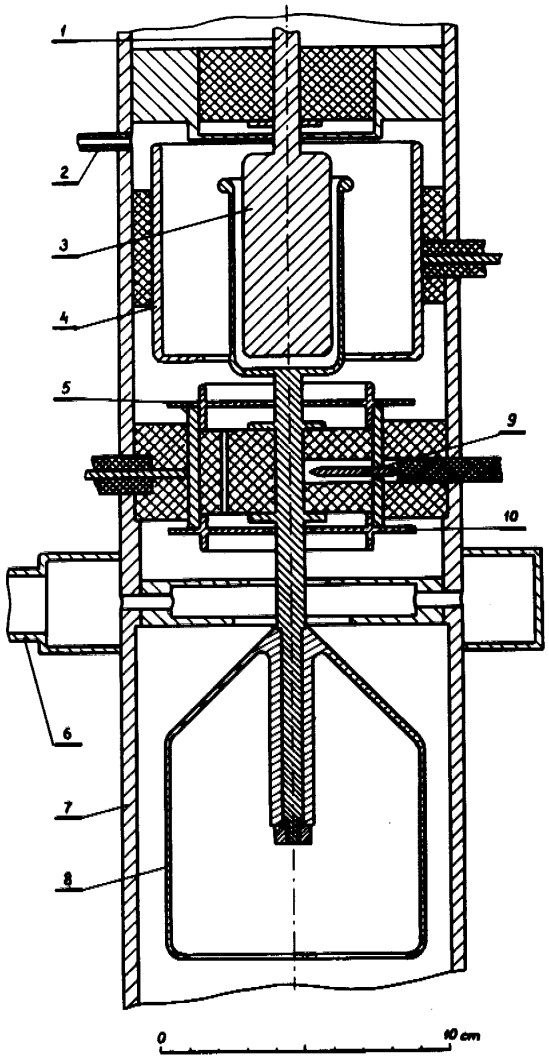

FIGURE 35.1. Schematic diagram of the measuring capacitor of the counter with combined circuit arrangement:

1 — branch to the electrometer; 2 — connecting branch for feeding dried air into the chamber of the insulators; 3 — cylinder of the dividing capacitor; 5 and 10 — screens of the insulator; 6 — branch for pumping out the air; 7 — outer cylinder; 8 — inner cylinder; 9 — switch K_2.

Teflon insulators have an extremely high resistance and are ideally moisture proof, but possess a high emf noise. The best insulating properties are exhibited by sapphire. A perfected design of sapphire insulators for a measuring capacitor is described in the paper /Gunn, 1965/. When designing counters for operation under extremely severe meteorological conditions it is also useful to consider the designs which have been developed for insulating field measuring devices of the collector type /Dolezalek, 1956, 1961; Gadomski, 1965/.

Currently, major effort is being put into the development of universal portable counters intended for the study of various artificial sources of air ions in addition to the study of the natural ionization of atmospheric air. The Israël counter /Israël, 1929/, which is manufactured to this day by Spindler and Choier (F. R. G.), can be considered as the first of the contemporary portable counters. The Israël counter uses two measuring capacitors — one for positive and one for negative air ions. When necessary, the measuring capacitors can be connected in series. The air-flow rate is low and the voltage of the measuring capacitor is relatively low. The two measuring capacitors are of the same size: $r_2 = 3.4$ cm, $r_1 = 2.6$ cm, $l = 50$ cm. A drawback of the Israël counter is the edge effect — the counter is connected according to the arrangement with a grounded inner collector plate and does not possess an electrostatic shield. The counters of Bogoyavlennyi /Lesgaft, 1938/ and Tverskoi /Tverskoi, Otto, 1962/ have similar properties. The latter is described in the paper /Styro, Yurgelionis, 1956/. The Tverskoi counter is equipped with one measuring capacitor for light ions and one for heavy ions. Flow rates of up to 600 cm^3/sec and voltages of up to 300 V are used. The effective capacitance of the measuring capacitor for light ions is 4 cm, and that of the measuring capacitor for heavy ions 105 cm. The instrument dimensions are 80×32×18 cm, and its weight is 16 kg. The simplified Tverskoi counter /Grachev, 1959/, intended for the measurement of light ions only, is even more compact.

Many designs of portable counters were developed by the group of collaborators of the Tartus State University under the direction of Reinet /Reinet, 1959b, 1962a, 1962b, 1963/. In the SAG-2M counter a mechanical electrometer of the type SG-1M is used. The edge effect is suppressed, since the measuring capacitor is connected according to the circuit arrangement with a grounded outer plate. In order to suppress the effect of random fluctuations of the supply voltage on the measurement results a bridge circuit is used. The design of the insulators prevents leakage and parasitic polarization phenomena. The dimensions of the measuring capacitor are $r_2 = 1.95$ cm, $r_1 = 0.95$ cm, $l = 63$ cm. The maximum voltage of the measuring capacitor is 300 volts, the maximum flow rate 600 cm^3/sec. The outside dimensions of the instrument are 85×43×33 cm; the weight is 31 kg.

The dynamic electrometer is used in the counter of Komarov, Kuzmenko and Seredkin /Komarov, Kuzmenko, and Seredkin, 1961/. The dimensions of the measuring capacitors of this counter are chosen on the basis of

theoretical calculations. The edge effect is suppressed by using an electrostatic shield. An improved variant of the bridge circuit was utilized. The rigid design of the measuring capacitors which enables the instrument to be used aboard aircraft deserves attention. The counter of Komarov, Kuzmenko and Seredkin is one of the most highly perfected contemporary counters. However, it is unique and is not manufactured industrially. A counter of the type SI-62 /Kitaev, Kloiz, 1963/ is manufactured in the Soviet Union. The design of this counter consists of elements of the counters of Reinet and of the counter of Komarov, Kuzmenko and Seredkin. The SI-62 counter is provided with two measuring capacitors connected according to the circuit arrangement with a grounded inner collector plate. The dimensions of both capacitors are identical: $r_2 = 1.9$ cm, $r_1 = 1.2$ cm, $l = 58$ cm. The voltage of the measuring capacitor can reach 250 volts and flow rates of up to 1500 cm/sec can be attained. The air-ion current is measured with the aid of a mechanical or cathode electrometer. The weight is 85 kg and the outside dimensions of the instrument are relatively large. A particular feature of the SI-62 counter is the presence of a portable measuring capacitor, which can be installed at a distance of up to 5 m from the remaining parts of the instrument. Royco Instruments, California, manufactures a model 411 light-ion counter and the model 412 counter, having a minimum limiting mobility of 0.0064 $cm^2/V \cdot sec$. The instruments manufactured by Royco are distinguished by the flat geometry of the plates of the measuring capacitor. Kathrein, West Germany, manufactures a model 8310 ionometer, which is characterized by a high sensitivity. The limiting mobility is fixed (0.9 $cm^2/V \cdot sec$). The inner plate of the cylindrical measuring capacitor of the model 8310 counter is tubular. 14% of the air flows through the inner plate and is not utilized for measurements. The demands laid down in § 3 are not satisfied. However, in the instrument model 8310 this does not cause any distortions.

A very compact recording counter of light ions is described in the paper /Giorgi, 1963/.

Several other extremely simplified designs of portable counters with small outside dimensions are known /Grachev, 1962; Derekhaov, 1962/. Their use is limited to checking the operation of artificial air-ion generators, used in medicine and industry. Several models of simplified counters are described in the paper /Livshitz, Moiseev, 1965/.

Special demands are made upon the design of counters for the study of the ionization of the free atmosphere. Counters intended for use aboard aircraft /Wigand, 1914, 1921; Gish, Sherman, 1935; Callahan, Fraucher, 1954; Coroniti, 1960; Kranopevtsev, 1966; Paltridge, 1966/ differ only slightly from standard counters. A particular feature of some instruments /Zachek, 1965/ is the use of special devices to effect a decrease in the compensation of the flow of particles which settle due to inertial forces. Counters used in radiosondes attached to free balloons should operate automatically and weigh not more than a few kilograms. In such counters one utilizes the natural ventilation, arising in a vertically mounted capacitor when the balloon ascends. Owing to the strict technical

demands, radiosondes merely enabled the simplest measurement in the range of high limiting mobilities/Venkiteshwaran, Gupta, Huddar, 1953; Koenigsfeld, 1955, 1957; Venkiteshwaran, 1958; Hatakeyama, Kobayashi, Kitaoka, Uchikawa, 1958; Woessner, Cobb, Gunn, 1958; Mühleisen, Fischer, 1958; Jones, Maddever, Sanders, 1959; Kroening, 1960; Coroniti, Mazarek, Stergis, Kotas, Seymour, Werme, 1954; Uchikawa, 1963, 1966; Paltridge, 1965; Takeuti, Ishikawa, Iwata, 1966; Pavlyuchenkov, 1966/. In the paper /Kroening, 1960/ a mechanical electrometer is used which at the same time serves as an automatic switch /Neher, 1953/. In all the remaining counters for radiosondes different variants of cathode electrometers are used and more rarely dynamic electrometers.

In the paper /Bordeau, Whipple, Clark, 1959/ a counter intended for use aboard a meteorological rocket is described.

In all the counters considered above the integral measuring method is used. Differential methods were used much more rarely. Apart from designs mentioned in the first chapter of the present work, the first-order differential counters described in the papers /De Broglie, 1909; Nolan, P. J., 1926; Young, 1926, Gagge, Moriyama, 1935; Misaki, 1961/ and second-order differential counters described in the papers /Chapman, 1937; Yunker, 1940; Daniel, Brackett, 1951; Hewitt, 1957; Hoegl, 1963a, b/ should be mentioned. The insulator design described in the work /Chapman, 1937/ is worthy of attention. In order to ensure a large leakage resistance under conditions of high humidity of the investigated air an auxiliary flow of dried air is used, which flows around the insulator. The counter described in the work /Hewitt, 1957/ is based on a special principle. In this instrument, the measured air ions do not settle in the capacitor, but are drawn through a narrow slit and are collected in an adsorbent filter which is connected to the electrometer. Here, disturbances caused by the instability of the voltage source are suppressed. This approach is utilized also in the paper /Wnitby, Clark, 1966/.

To measure the space charge density, the method of the adsorption filter is most widespread. Apart from instruments mentioned in the first chapter, space charge counters are described in the papers /Dowling, Haughey, 1922; Wolodkewitsch, Dessauer, 1931a; Pluvinage, 1946; Beau, Blanquet, L., Blanquet, P., 1953; Beau, Blanquet, L., Blanquet, P., Fourton, 1956; Gonsior, 1957; Makhotkin, Sushchinskii, 1960; Moore, Vonnegut, Mallahan, 1961; Arabadzhi, Rudik, 1963; Bent, 1964/. The instrument described in the last paper is distinguished by a highly perfected insulator design and high sensitivity (air-flow rate 3000 cm^3/sec) /Arabadshi, Rudik, 1963/. The highest sensitivity in charge density measurements was attained in the study /Moore, Vonnegut, Mallahan, 1961/, where a filter is described which is capable of letting through an air flow with a flow rate of up to 0.7 m^3/sec.

§36. DESCRIPTION OF A UNIVERSAL INTEGRAL AIR-ION COUNTER

The counter described below (SAI-TGU-66) was designed and built by the staff of the Tartu State University under the direction of the author.

This counter is the last model of a series of constantly improved counters SAI-TGU-64, SAI-TGU-65, SAI-TGU-65 m.

The design was implemented with the aim of ensuring small outside dimensions of the instrument and operating convenience.

The measuring capacitor of the counter is connected according to the circuit with a grounded outer collector plate. The design specifications of the measuring capacitor were calculated accordingly (Figure 36.1). The capacitor is mounted vertically with the entrance opening facing upward. The outer plate (7) is connected to the voltage source via a lower terminal. The terminal is connected to the inner plate by means of a lead, drawn tightly along the axis of the grounded supporting tube. The centering system of the inner plate (8) has 6 degrees of freedom. After all the adjustments are made the system is secured with the aid of epoxy glue. The outer plate (5) is carefully insulated.

The lead of the outer plate through the annular insulator (6) is not shown in the figure. In order to suppress turbulent mixing the outer plate is given a conical form. The conicity is not large and amounts to 1:50. The cross section of the air flow is narrowed down by 30% along the entire length of the inner plate. The inlet opening of the inner plate (2) is covered by a grid (3) of mesh width $h = 2$ mm and made of wire of $r_0 = 50\mu$. The grid shields the conical inlet tube against the inner plate. Apart from this, the grid prevents the entry of insects into the measuring capacitor, guards against accidental touching of the inner plate, which is maintained at high voltage, and suppresses to some extent the turbulence of the incoming air. At a flow rate of 4500 cm^3/sec the adsorption of light ions on the grid is 2 – 3%.

The measuring capacitor can be readily disassembled. After unscrewing the upper shielding tubes (4) the outer plate together with the plastic annular insulator (6) are easily taken out. When it is necessary to separate the inner plate, it suffices to unscrew one bolt and to lift up the plate. After dismounting, all insulators and the plate surfaces are accessible for cleaning. In order to clean the grid of adhering particles, one can hold the removed outer plate upside down (with the grid facing downward) under a water tap with a strong, wide, foamy stream. The grid and the plate of the measuring capacitor are made of aluminum alloys. The capacitance of the measuring capacitor is 51 pF. The effective capacitance of the precondenser is 1 pF. The inner plate of the measuring capacitor (1) is removable and the entrance tube is the outer plate (2).

The block diagram of the counter is shown in Figure 36.2. At the input of the electrometer a dynamic capacitor C_2 is used which modulates the constant signal with a frequency of 425 Hz. The dynamic, small-size capacitor designed by O. V. Saks ensures a modulation coefficient of 0.4 under these operating conditions. The alternating component of the voltage is transmitted from the dynamic capacitor to the amplifier through a double dividing capacitor C_3, C_4. The dividing capacitor has a special design with a guard ring, preventing the self-discharge of the capacitor C_3 on the surfaces of the insulator. The dielectric of the dividing capacitor is a

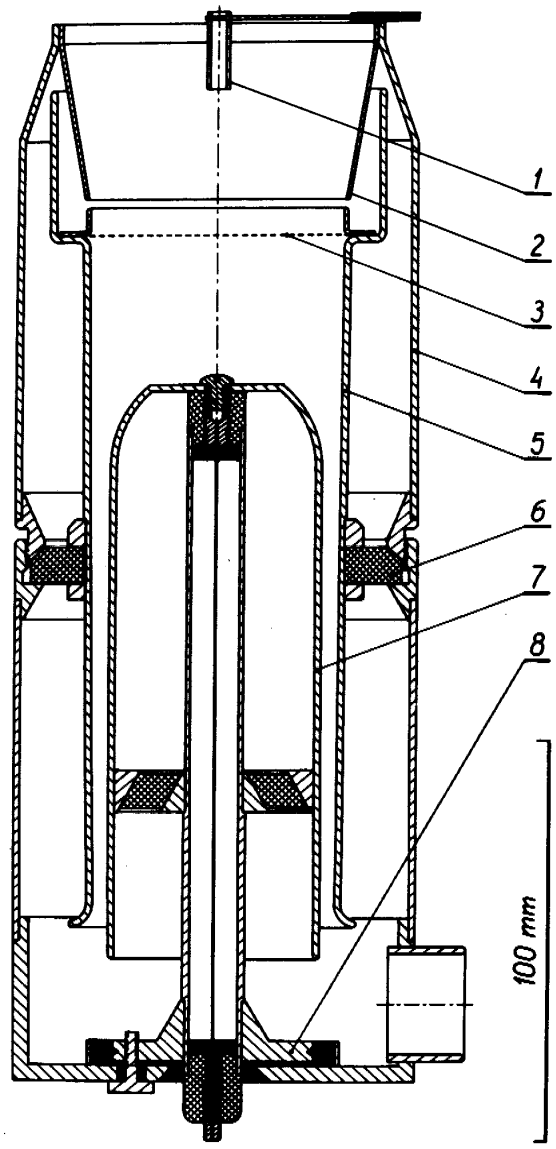

FIGURE 36.1. Measuring capacitor of the SAI-TGU-66 counter.

fluoroplastic film. The constant-voltage signal is amplified 10,000-fold from the dynamic capacitor to the output of the amplifier. From the divider $R_a - R_b$, a 40—120-fold feedback is applied to the input through the resistance R_s. At full scale the voltage across the terminals of the resistor R varies from 70 to 228 millivolts. The voltage between the outer plate and air is only 1.5 millivolts. The electrometer operates as an analog amplifier with a potentially grounded input. The current generated by the air ions is compensated by the current through the resistance R. This system of feedback renders the measurement accuracy practically independent of the drift of the amplifying coefficients of the tubes and also effects a 40—120-fold reduction in the leakage resistance caused by the shunting effect of the insulators of the outer plate.

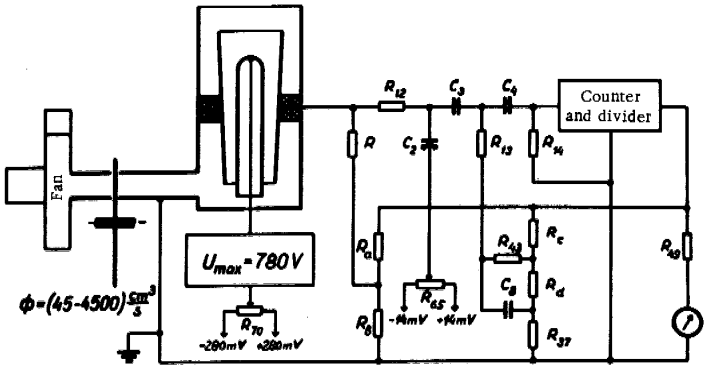

FIGURE 36.2. Block diagram of the SAI-TGU-66 counter.

The shunting effect of the leakage resistance under such conditions is not dangerous. Dirt accumulation becomes marked already at leakage resistance, the shunting effect of which is not felt.

The resistance R is connected depending on the measuring range of the conditional charge density. The largest value is $R=10^{12}$ ohm; the smallest is $R=10^{7}$ ohm.

Feedback is also utilized for the control of the degree of smoothing of the recording of the conditional charge density with time. The smoothing is carried out by an integrating circuit, consisting of resistances R, R_{12}, and the capacitor C_3. An additional feedback signal from the divider $R_c - R_d - R_{37}$ is applied through the capacitor C_3. The auxiliary circuit $R_{43}C_8$ serves for the stabilization of the transient process. The time constant of the transient process depends on the position of the switches, reversing the outlet of the divider $R_c - R_d$ and the resistance R. In the case $R=10^{12}$ ohm the shortest time required to attain 90% of full scale is 35 sec. The largest time constant of smoothing is 1500 sec. In the case $R \leqslant 3.3 \cdot 10^{9}$ ohm these quantities are 2 and 140 sec, respectively.

The potentiometer R_{65} serves to determine the zero of the electrometer. The potentiometer R_{70} serves for the compensation of the contact potential between the plates of the measuring capacitor.

Figure 36.2 shows the block diagram of the air path, consisting of the measuring capacitor, the switch of the diaphragm and the fan. By switching in the calibrated diaphragms flow rates of 45, 142, 450, 1420, or 4500 cm^3/sec can be achieved.

The entire circuit diagram of the counter is shown in Figure 36.3. Data of the circuit are listed in the specifications at the end of the present section.

The power transformer of the counter operates under conditions of ferroresonance, which ensures the stabilization of all voltages in the circuit. The voltage of the inner plate of the measuring capacitor is stabilized in addition by a 2-step stabilizer using SG-303S and SG-301S voltage regulators. The output voltage regulators V_5 and V_6 operate under optimum current conditions (about 14 μA), thermal insulation and mechanical shock absorbers. The attenuator $R_{88} - R_{91}$ and the divider $R_{78} - R_{87}$ are built from stable microwire resistors.

The amplifier of the electrometer consists of an amplification of the alternating current at the pentode V_1, a phase detector at the pentode with two grids V_2, and a series-ballanced amplifier of constant current at the double triode V_4. The pentode V_3 serves as an oscillator for the dynamic capacitor. The magnetizing current for the winding W is stabilized by a 12-fold negative feedback of the constant-current oscillator.

The counter is supplied by an external automatic blocking system, consisting of a relay Rel connected via the bridge $D_6 - D_9$, a limiter $D_2 - D_5$ and the pulse-linked capacitors C_9 and C_{33}. The relay Rel consists of a standard 2-way polarizing relay of the type RP-4. If the moving contact of the relay is in the left-hand position, then the input of the electrometer is shorted. The position of the relay Rel may be judged from the signal lamp L_1. The relay is operated by hand with the aid of the switch S_0. Automatic triggering of the relay occurs in the case of a constant 160% overload of the electrometer when a pulse signal appears on the grid of the tube V_4. The pulse signal arrives on the grid V_4 via a capacitor C_{33} when the voltage of the measuring capacitor is reversed. The high-speed external blocking system prevents high voltages from reaching the outer plate of the measuring capacitor, which in the case of improper operation of the instrument could polarize the insulator and put the instrument out of order for a long time.

The operation of the counter is very simple, since in order to determine the limiting mobility and the range of the conditional concentration, the reading on the counter is merely multiplied.

Let us state some other data on the SAI-TGU-66 counter.

1. The limiting mobility has all told 50 nominal values, determined by the switches. These values are: 8; 6.3; 5; 4; 3.2; 2.5; 1.6; 1.26; 1; 0.8; 0.63; .....; 0.00016; 0.000123; and 0.0001 ($cm^2/V \cdot sec$). The maximum voltage of the measuring capacitor is 780 volts.

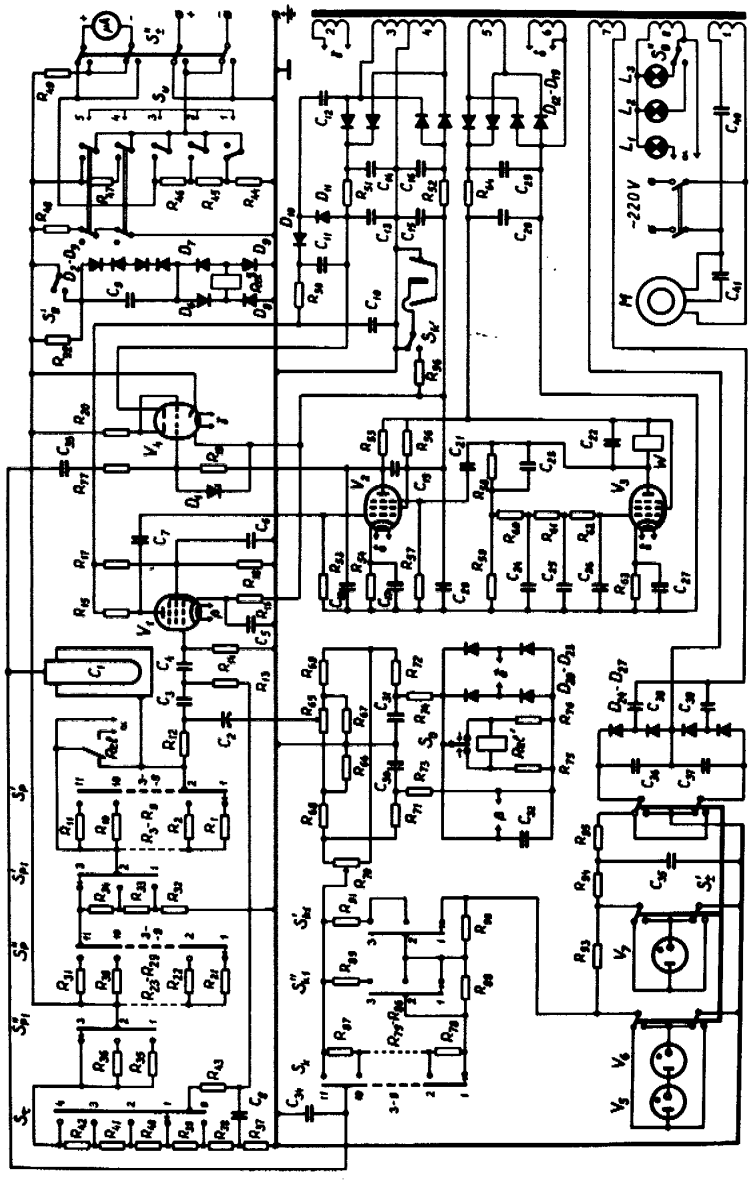

FIGURE 36.3. Circuit diagram of the SAI-TGU-66 counter.

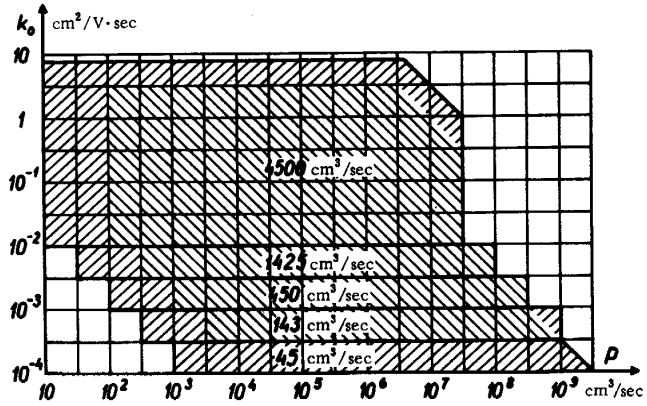

FIGURE 36.4. Measurement limits of the SAI-TGU-66 counter. The hatchings in the other direction correspond to the region in which marked distortions are possible.

2. There are 35 possible ranges of the conventional concentration of the charge with upper limits 100; 200; 316; 632; 1000; ..... 10^9, 2×10^9, 3.16×10^9 (elementary charges/cm³).

3. The actual measurement limits are shown in Figure 36.4.

4. $s_{\tau UC}$ (40 sec) $\approx 10^{-6}$; $\sigma_{UE} \approx 40$ μV; $\sigma_{UR}/R_p \approx 10^{-16}$ A.

5. For light ions $\sigma_p < 10$ elementary charges/cm³, for $k_0 = 0.0005$ cm²/V·sec $\sigma_p < 400$ elementary charges/cm³.

6. The constant of the edge effect is $C/C_1 = 25{,}000$.

7. The counter is provided with a preliminary capacitor having an electric switch. The limiting mobility of the preliminary capacitor at $\Phi = 142$ cm³/sec is 0.12 cm²/V·sec.

8. To the counter we can connect a potentiometric recorder with an input of 10, 100, or 150 mV, or a recording voltmeter with 15V full-scale deflection and a current consumption up to 5 mA. There is also a standard current output up to 5 mA for a load of 2.4 kohm for automatic control devices.

9. The mean measurement error is not higher than 5%.

10. The outside dimensions of the counter (in portable state) are 45 × 23 × 33 cm; the weight does not exceed 12 kg. The required power is not more than 45 watts.

The counter is illustrated in Figure 36.5.

Design specifications for Figure 36.3

I. VACUUM-TUBE AND SEMICONDUCTOR ELEMENTS

V_1 and V_3	V_2	V_4	V_5 and V_6	V_7	$L_1 - L_3$
6Zh 1 P	6Zh 2P	6 N 14P	SG-301 S	SG-303 S	LN3.5—0.28

$D_1 - D_5$	$D_6 - D_{19}$	$D_{20} - D_{23}$	$D_{24} - D_{27}$
D 810	D 226 B	D 7 A	AVS-1-220

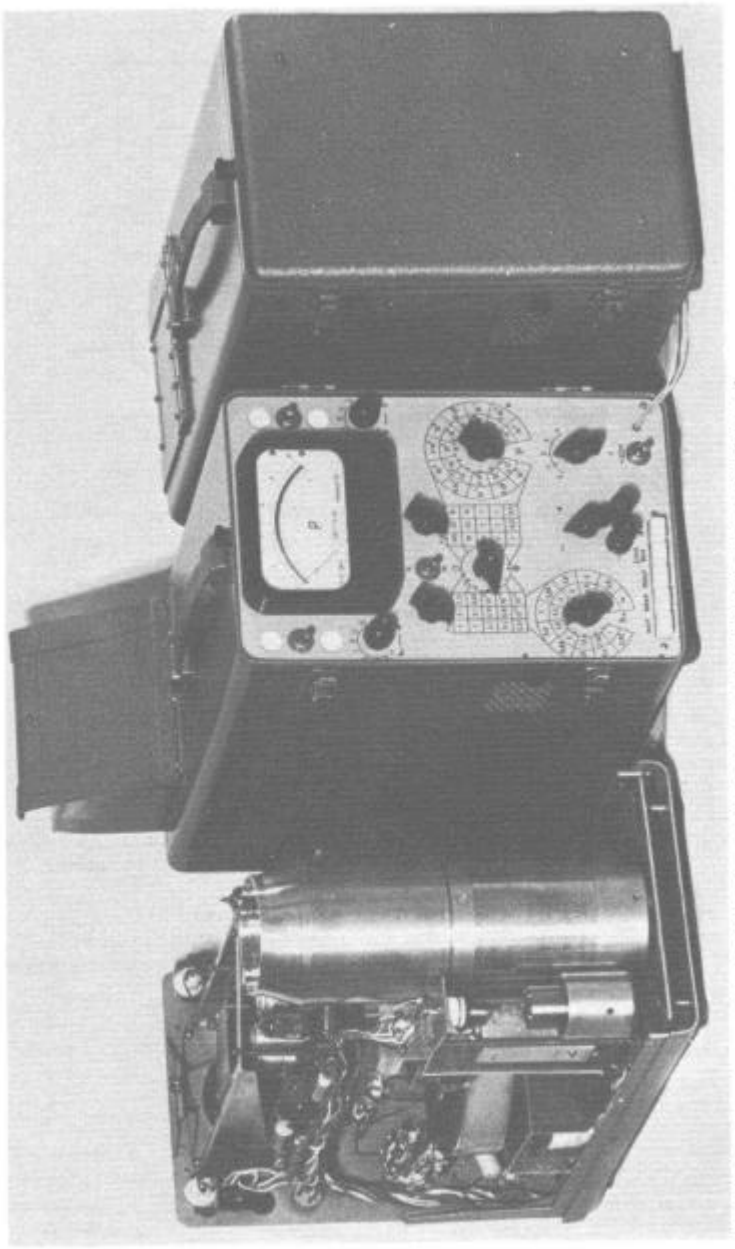

FIGURE 36.5. Three forms of the SAI-TGU-66 counter (with cover removed, in working state, in portable state).

II. CAPACITORS

No.	C	Type	No.	C	Type
1	51	Measuring	22	0.07	KBGI – 200 V
2	25	Dynamic	23	0.05	MBM – 160 V
3	20	Dividing	24	2000	KSO – 500 V
4	40	"	25	2000	"
5	0.25	MBM – 160 V	26	2000	"
6	0.05	"	27	20.0	K50 – 3 – 25 V
7	2000	KSO – 500 V	28	20.0	KE – 2 – 150 V
8	1.0	MBM – 160 V	29	50.0	"
9	1.0	"	30	20.0	K50 – 3 – 6 V
10	0.25	MBM – 500 V	31	20.0	"
11	5.0	KE – 2 – 300 V	32	400.0	ETO – 15 V
12	0.25	MBM – 500 V	33	390	POV – 10 kV
13	20.0	K50 – 3 – 160 V	34	390	"
14	50.0	"	35	0.1	MBM – 1500 V
15	20.0	"	36	0.1	MBM – 1000 V
16	50.0	"	37	0.1	MBM – 1500 V
17	20.0	K50 – 3 – 6V	38	0.25	MBM – 500 V
18	1.0	MBM – 160 V	39	0.25	"
19	1.0	"	40	1.0	MBGCh – 750 V
20	1.0	"	41	2.0	MBGCh – 250 V
21	4700	BM – 200 V			

III. RESISTORS

No.	R	Type	No.	R	Type
1	1000G	KVM	25	33k	MLT – 0.5
2	330G	"	26	33k	"
3	100G	"	27	33k	"
4	33G	"	28	33k	"
5	10G	"	29	33k	"
6	3.3G	"	30	33k	"
7	1G	"	31	33k	"
8	330.0	"	32	158.5Ω	wire
9	100.0	"	33	161	"
10	33.0	"	34	187	"
11	10.0	MBM – 1000 V	35	0.36	MLT – 0.5
12	100G	KLM	36	0.1	"
13	330.0	KIM – 0.125	37	1k	"
14	330.0	"	38	1k	"
15	4.7	"	39	3.6k	"
16	1.5	"	40	12k	"
17	4.7	"	41	36k	"
18	1.0	"	42	0.12k	"
19	1.0	"	43	4.7	"
20	1k	"	44	100	wire
21	33k	"	45	900	"
22	33k	"	46	500	"
23	33k	"	47	600	"
24	33k	"	48	3.6k	MLT – 0.5

III. RESISTORS (cont.)

No.	R	Type	No.	R	Type
49	0.148	MVSG – 0.5	73	2.4 k	MLT – 0.5
50	0.24	MLT – 0.5	74	2.4 k	"
51	1 k	"	75	3.6 k	"
52	1 k	"	76	3.6 k	"
53	15.0	KIM 0.125	77	1.0	"
54	3.6 k	MLT – 0.5	78	4.58**	MVSG – 0.5
55	0.47	"	79	3.64**	"
56	0.36	"	80	2.89**	"
57	0.12	"	81	2.29	"
58	2.0	"	82	1.82	"
59	0.36	"	83	1.445	"
60	0.27*	"	84	1.149	"
61	0.36	"	85	0.911	"
62	0.36*	"	86	0.725	"
63	2.4 k	"	87	2.80	"
64	1 k	"	88	20.0**	"
65	220	SPO – 0.5	89	2.47	"
66	100	MLT – 0.5	90	20.0**	"
67	100	"	91	2.47	"
68	1 k	"	92	1.5	"
69	1 k	"	93	9.4**	MLT – 0.5
70	1 k	SPO – 0.5	94	2.0	"
71	1 k	MLT – 0.5	95	4.0**	"
72	1 k	"	96	0.1	"

IV. ELECTROMAGNETIC ELEMENTS

R – relay built from RP-4, 6 kohm windings
L – winding of the dynamic capacitor
M – synchronous electric motor G – 31 A
A – instrument M 265, 100 μA

V. WINDINGS OF THE TRANSFORMER

1 – 2400 × PEL 0.21
2 – 46 × PEL 0.51
3 – 700 × PEL 0.07
4 – 700 × PEL 0.07
5 – 750 × PEL 0.10
6 – 46 × PEL 0.25 × 2
7 – 3000 × PEL 0.05
8 – 25 × PEL 0.25 × 3

The designations are given in order of spacing of the windings.

Between the windings 1 – 2, 4 – 5, 6 – 7, 7 – 8, a fluoroplastic insulator was placed.

* More accurate upon adjustment.
** Two equal resistors in series.